TABLE 3

Subgroup analysis in the malignant group (Grades II & III) for 1p LOH, p73, and RASSF1A promoter methylation according to patient age, sex, and tumor location

Factor	1p LOH (%)	*p73* Promoter Methylation (%)	*RASSF1A* Promoter Methylation (%)
age in yrs			
<50	4 of 5 (80)	4 of 5 (80)	3 of 5 (60)
≥50	11 of 13 (84.6)	10 of 13 (76.9)	7 of 13 (53.8)
p value	0.827	0.8961	0.827
sex			
F	9 of 11 (81.8)	9 of 11 (81.8)	5 of 11 (45.5)
M	6 of 7 (85.7)	5 of 7 (71.4)	5 of 7 (71.4)
p value	0.8408	0.6301	0.503
location			
convexity	9 of 10 (90)	9 of 10 (90)	3 of 10 (30)
other	6 of 8 (75)	5 of 8 (62.5)	7 of 8 (87.5)
p value	0.4262	0.1829	0.0125*

* Significant according to analysis of variance.

Chromosome 1p36 contains many genes of biological interest. The *p73* gene is a member of the *p53* family and is located on 1p36.33. Loss of *p73* expression has been observed at the RNA and protein levels in various human primary tumors and in cell lines derived from these tumors;[7,13,17] however, mutations or homozygous deletions are either absent or very rare. Transcription of *p73* is regulated by its promoter and the flanking exon 1, which is rich in CpG dinucleotides and contains putative binding sites for Sp1, Ap-2, Egr-1, Egr-2, and Egr-3.[1] Methylation of *p73* has been observed in approximately 30% of primary acute lymphoblastic leukemias and Burkitt lymphomas;[7] it may be implicated in the tumorigenesis and malignant transformation of meningiomas. In our study, *p73* methylation was detected in 14 (77.8%) of 18 of the malignant tumors, whereas it was absent in the benign tumors. Of the 15 malignant meningiomas with the 1p deletion, 14 exhibited *p73* methylation. Based on our data, we suggest that meningioma progression from the benign to the atypical state might be associated with 1p LOH and *p73* methylation.

The *RASSF1A* gene is a candidate tumor suppressor gene that was isolated from a 120-kb region of the minimal homozygous deletion on 3p21.3. The *RASSF1A* gene encodes a 340 amino acid protein that is predicted to contain a distal Ras-association domain.[8] Furthermore, this protein is also predicted to contain an NH_2-terminal diacylglycerol-binding domain and a PEST domain; these domains are commonly found in proteins that are regulated by ubiquitin-mediated proteolysis.[6] The PEST domain contains a phosphoserine residue that is phosphorylated in vitro by ataxia telangiectasia–mutated and related protein kinases.[18] Further studies are definitely necessary to elucidate the function of *RASSF1A*, and studies are underway to determine its role in meningioma tumorigenesis. The *RASSF1A* gene is frequently inactivated in various cancers by promoter hypermethylation. It is well known that promoter hypermethylation prevents *RASSF1A* expression in glioma and medulloblastoma cell lines. Horiguchi et al.[12] used methylation-specific PCR to analyze the methylation status of the *RASSF1A* promoter in 73 primary brain tumors and four glioma cell lines; they detected *RASSF1A* methylation in 25 (54.3%) of 46 gliomas and in all five medulloblastomas studied. Typically, *RASSF1A* methylation is more frequently detected in Grades II and III gliomas than in glioblastoma multiforme. This relatively high frequency of *RASSF1A* promoter methylation observed in lower-grade gliomas may correspond to an early event during glioma progression. Glioblastoma multiforme is considered to manifest as a primary (de novo) or a secondary tumor.[23] Although these tumors have a common phenotypic end point, they are generally believed to arise via different genetic pathways; thus, primary and secondary glioblastomas are considered to originate from genetically distinct disease entities. Therefore, *RASSF1A* methylation may be involved in the formation and progression of a specific tumor. In our study, *RASSF1A* promoter methylation was detected in four (18.2%) of 22 of the benign tumors; this was consistent with a previous report in which *RASSF1A* methylation was demonstrated in two (16.7%) of 12 meningiomas.[12] Further, we detected *RASSF1A* methylation in 10 (55.6%) of 18 of the malignant tumors. Thus, similar to gliomas, malignant meningiomas may also arise via several different genetic pathways.

A unique feature of this study was that it included malignant meningiomas that recurred from Grade I tumors. Of the 37 meningiomas, nine were recurrent; moreover, eight (88.9%) of nine belonged to the malignant category and only one (4.5%) of 22 cases to the benign category. We analyzed three of the patients with recurrent tumors. An interesting observation in the case that is presented in Fig. 1 was that 1p LOH was detected in the Grade III recurrent tumor (number 34R) but not in the primary Grade I tumor (number 22). These data strongly support our hypothesis that meningioma progression from the benign to the atypical state is related to 1p LOH and *p73* methylation. Nevertheless, the cause of these genetic alterations and the mechanism underlying tumor progression remain unclear. The study of a larger number of malignantly transformed meningiomas could enable the elucidation of these issues.

Conclusions

Additional genetic alterations following an initial alteration may give rise to a larger number of rapidly growing tumor cells that are identified by a high MIB-1 index. Tumors progress by a multistep process by the cumulative acquisition of genetic alterations. Based on the results in this study, we suggest that meningiomas similarly progress from the benign to the malignant state by the accumulation of genetic alterations such as 1p LOH and *p73/RASSF1A* promoter methylation. Ultimately, this type of genetic fingerprint may play both diagnostic and therapeutic roles.

Acknowledgments

The first two authors contributed equally to the work on this report.

References

1. Banelli B, Casciano I, Romani M: Methylation-independent silencing of the p73 gene in neuroblastoma. **Oncogene 19:** 4553–4556, 2000
2. Baser ME, Poussaint TY: Age associated increase in the prevalence of chromosome 22q loss of heterozygosity in histological subsets of benign meningioma. **J Med Genet 43:**285–287, 2006

3. Bello MJ, de Campos JM, Vaquero J, Kusak ME, Sarasa JL, Rey JA: High-resolution analysis of chromosome arm 1p alterations in meningioma. **Cancer Genet Cytogenet 120:**30–36, 2000
4. Boström J, Meyer-Puttlitz B, Wolter M, Blaschke B, Weber RG, Lichter P, et al: Alterations of the tumor suppressor genes CDKN2A (p16(INK4a)), p14(ARF), CDKN2B (p15(INK4b)), and CDKN2C (p18(INK4c)) in atypical and anaplastic meningiomas. **Am J Pathol 159:**661–669, 2001
5. Bostrom J, Muhlbauer A, Reifenberger G: Deletion mapping of the short arm of chromosome 1 identifies a common region of deletion distal to D1S496 in human meningiomas. **Acta Neuropathol 94:**479–485, 1997
6. Burbee DG, Forgacs E, Zochbauer-Muller S, Shivakumar L, Fong K, Gao B, et al: Epigenetic inactivation of RASSF1A in lung and breast cancers and malignant phenotype suppression. **J Natl Cancer Inst 93:**691–699, 2001
7. Corn PG, Kuerbitz SJ, van Noesel MM, Esteller M, Compitello N, Baylin SB, et al: Transcriptional silencing of the p73 gene in acute lymphoblastic leukemia and Burkitt's lymphoma is associated with 5' CpG island methylation. **Cancer Res 59:**3352–3356, 1999
8. Dammann R, Li C, Yoon JH, Chin PL, Bates S, Pfeifer GP: Epigenetic inactivation of a RAS association domain family protein from the lung tumor suppressor locus 3p21.3. **Nat Genet 25:** 315–319, 2000
9. Dumanski JP, Carlbom E, Collins VP, Nordenskjold M: Deletion mapping of a locus on human chromosome 22 involved in the oncogenesis of meningioma. **Proc Natl Acad Sci U S A 84:** 9275–9279, 1987
10. Herman JG, Baylin SB: Gene silencing in cancer in association with promoter hypermethylation. **N Engl J Med 349:**2042–2054, 2003
11. Hibi K, Robinson CR, Booker S, Wu L, Hamilton SR, Sidransky D, et al: Molecular detection of genetic alterations in the serum of colorectal cancer patients. **Cancer Res 58:**1405–1407, 1998
12. Horiguchi K, Tomizawa Y, Tosaka M, Ishiuchi S, Kurihara H, Mori M, et al: Epigenetic inactivation of RASSF1A candidate tumor suppressor gene at 3p21.3 in brain tumors. **Oncogene 22:** 7862–7865, 2003
13. Ichimiya S, Nimura Y, Kageyama H, Takada N, Sunahara M, Shishikura T, et al: p73 at chromosome 1p36.3 is lost in advanced stage neuroblastoma but its mutation is infrequent. **Oncogene 18:** 1061–1066, 1999
14. Issa JP: CpG island methylator phenotype in cancer. **Nat Rev Cancer 4:**988–993, 2004
15. Jones PA, Baylin SB: The fundamental role of epigenetic events in cancer. **Nat Rev Genet 3:**415–428, 2002
16. Kaghad M, Bonnet H, Yang A, Creancier L, Biscan JC, Valent A, et al: Monoallelically expressed gene related to p53 at 1p36, a region frequently deleted in neuroblastoma and other human cancers. **Cell 90:**809–819, 1997
17. Kawano S, Miller CW, Gombart AF, Bartram CR, Matsuo Y, Asou H, et al: Loss of p73 gene expression in leukemias/lymphomas due to hypermethylation. **Blood 94:**1113–1120, 1999
18. Kim ST, Lim DS, Canman CE, Kastan MB: Substrate specificities and identification of putative substrates of ATM kinase family members. **J Biol Chem 274:**37538–37543, 1999
19. Lee JY, Finkelstein S, Hamilton RL, Rekha R, King JT Jr, Omalu B: Loss of heterozygosity analysis of benign, atypical, and anaplastic meningiomas. **Neurosurgery 55:**1163–1173, 2004
20. Lekanne Deprez RH, Bianchi AB, Groen NA, Seizinger BR, Hagemeijer A, van Drunen E, et al: Frequent NF2 gene transcript mutations in sporadic meningiomas and vestibular schwannomas. **Am J Hum Genet 54:**1022–1029, 1994
21. Lomas J, Aminoso C, Gonzalez-Gomez P, Eva Alonso M, Arjona D, Lopez-Marin I, et al: Methylation status of TP73 in meningiomas. **Cancer Genet Cytogenet 148:**148–151, 2004
22. Lomas J, Bello MJ, Arjona D, Gonzalez-Gomez P, Alonso ME, de Campos JM, et al: Analysis of p73 gene in meningiomas with deletion at 1p. **Cancer Genet Cytogenet 129:**88–91, 2001
23. Maher EA, Furnari FB, Bachoo RM, Rowitch DH, Louis DN, Cavenee WK, et al: Malignant glioma: genetics and biology of a grave matter. **Genes Dev 15:**1311–1333, 2001
24. Meese E, Blin N, Zang KD: Loss of heterozygosity and the origin of meningioma. **Hum Genet 77:**349–351, 1987
25. Menon AG, Rutter JL, von Sattel JP, Synder H, Murdoch C, Blumenfeld A, et al: Frequent loss of chromosome 14 in atypical and malignant meningioma: identification of a putative 'tumor progression' locus. **Oncogene 14:**611–616, 1997
26. Modha A, Gutin PH: Diagnosis and treatment of atypical and anaplastic meningiomas: a review. **Neurosurgery 57:**538–550, 2005
27. Papi L, De Vitis LR, Vitelli F, Ammannati F, Mennonna P, Montali E, et al: Somatic mutations in the neurofibromatosis type 2 gene in sporadic meningiomas. **Hum Genet 95:**347–351, 1995
28. Piaskowski S, Rieske P, Szybka M, Wozniak K, Bednarek A, Pluciennik E, et al: GADD45A and EPB41 as tumor suppressor genes in meningioma pathogenesis. **Cancer Genet Cytogenet 162:**63–67, 2005
29. Ruttledge MH, Andermann AA, Phelan CM, Claudio JO, Han FY, Chretien N, et al: Type of mutation in the neurofibromatosis type 2 gene (NF2) frequently determines severity of disease. **Am J Hum Genet 59:**331–342, 1996
30. Sanson M, Cornu P: Biology of meningiomas. **Acta Neurochir (Wien) 142:**493–505, 2000
31. Versteeg R, Caron H, Cheng NC, van der Drift P, Slater R, Westerveld A, et al: 1p36: every subband a suppressor? **Eur J Cancer 31A:**538–541, 1995
32. Weber RG, Bostrom J, Wolter M, Baudis M, Collins VP, Reifenberger G, et al: Analysis of genomic alterations in benign, atypical, and anaplastic meningiomas: toward a genetic model of meningioma progression. **Proc Natl Acad Sci U S A 94:** 14719–14724, 1997
33. Wellenreuther R, Kraus JA, Lenartz D, Menon AG, Schramm J, Louis DN, et al: Analysis of the neurofibromatosis 2 gene reveals molecular variants of meningioma. **Am J Pathol 146:**827–832, 1995
34. Zang KD: Meningioma: a cytogenetic model of a complex benign human tumor, including data on 394 karyotyped cases. **Cytogenet Cell Genet 93:**207–220, 2001

Manuscript submitted September 27, 2006.
Accepted February 14, 2007.

Address reprint requests to: Jun Yoshida, M.D., Ph.D., Department of Neurosurgery, Nagoya University School of Medicine, 65 Tsurumai, Showa-ku, Nagoya 466–8550, Japan. email: jyoshida@med.nagoya-u.ac.jp.

Available online at www.sciencedirect.com
ScienceDirect
Neuroscience Letters 426 (2007) 69–74
Neuroscience Letters
www.elsevier.com/locate/neulet

Intravenously transplanted human neural stem cells migrate to the injured spinal cord in adult mice in an SDF-1- and HGF-dependent manner

Hiroki Takeuchi [a,1], Atsushi Natsume [a,1], Toshihiko Wakabayashi [b], Chihiro Aoshima [a], Shinji Shimato [b], Motokazu Ito [a], Jun Ishii [a], Yuka Maeda [a], Masahito Hara [a], Seung U. Kim [c,*], Jun Yoshida [a,b,**]

[a] *Department of Neurosurgery, Nagoya University School of Medicine, Nagoya, Japan*
[b] *Center for Genetic and Regenerative Medicine, Nagoya University Hospital, Nagoya, Japan*
[c] *Division of Neurology, Department of Medicine, University of British Columbia, Vancouver, Canada*

Received 17 June 2007; received in revised form 10 August 2007; accepted 21 August 2007

Abstract

Neural stem cell (NSC) transplantation has exhibited considerable therapeutic potential in spinal cord injury. However, most experiments in animals have been performed by injecting these cells directly into the injured spinal cord. A cardinal feature of NSCs is their exceptional migratory ability through the nervous system. Based on the migratory ability of NSCs, we investigated whether minimally invasive intravenous delivery of NSCs could facilitate their migration to the injured spinal cord and identified the chemo-attractants secreted by the lesions. Nude mice were injected intravenously with labelled human NSCs at 3, 7 and 10 days after the compression of the spinal cord at the T8 level. The migration of NSCs to the lesioned spinal cord was highest at 7 days after injury; this correlated with the peak of hepatocyte growth factor and stromal cell-derived factor-1 mRNA expressions in the lesion but not with the disruption of the blood–brain barrier. Finally, the grafted NSCs differentiated into neuronal and glial subpopulations at 21 days after transplantation. Our study suggests that intravenously administered NSCs can be employed as a renewable source for replacing lost cells for the treatment of spinal cord injuries.

Keywords: Spinal cord injury; Neural stem cells; Intravenous delivery; SDF-1; HGF

Neurogenesis following injury to the human adult central nervous system (CNS) is rare. Important advances have been made in understanding the conditions that influence the survival and regrowth of neurons following injury to mature CNS tissue. These conditions include the presence of neurotrophic factors or anti-apoptotic agents that promote survival and neuronal growth and enable the neural tissues to provide cellular scaffolds for axonal regeneration. Another approach to addressing CNS tissue injury is replacing lost cells, particularly neurons, with differentiating neural stem cells (NSCs). Stem cell therapy has considerable therapeutic potential in spinal cord injury [2,19]. However, recent stem cell transplantations have been performed mainly by direct surgery [20] or lumbar puncture [3]. The direct injection of stem cells by lumbar puncture into the central parenchyma of the patient's injured spinal cord is difficult to translate into clinical practice [13]. It might cause further deterioration by damaging the remaining healthy cord tissue or producing procedure-related complications in a patient with spinal cord injury. Furthermore, direct parenchymal cell transplantation prohibits the delivery of multiple dosages of therapeutic cells. Intriguingly, a cardinal feature of NSCs is their exceptional migratory ability. Their migratory capacity is emerging as a therapeutic paradigm in the treatment of various animal models of neurodegeneration, stroke and brain tumours [1,22,24,26]. Previously, in animal models of brain ischemia, cerebral haemorrhage and brain tumours, our group and others have reported that intravenously delivered F3 NSCs migrate into lesion sites, differentiate into neurons and glial cells and therapeutically affect functional improvement and tumour reduction [5,7,14].

* Co-corresponding author.
** Corresponding author at: Department of Neurosurgery, Nagoya University School of Medicine, 65 Tsurumai-cho, Showa, Nagoya 466-8550, Japan. Tel.: +81 52 744 2355; fax: +81 52 744 2361.
E-mail addresses: sukim@interchange.ubc.ca (S.U. Kim), nsoffice@med.nagoya-u.ac.jp (J. Yoshida).
[1] These authors contributed equally to this work.

0304-3940/$ – see front matter © 2007 Elsevier Ireland Ltd. All rights reserved.
doi:10.1016/j.neulet.2007.08.048

Based on NSC migratory ability, we investigated whether minimally invasive intravenous NSC delivery facilitates their migration to the injured spinal cord and identified chemoattractants secreted by the lesions.

Immortalised human NSCs have been established from embryonic human telencephalon tissues at 14 weeks gestation by transfection with a retroviral vector encoding the v-*myc* oncogene, as described previously [10,21]. One of the stable clonal NSC lines, HB1.F3, carries the normal human karyotype 46XX and self-renews and differentiates into neuronal and glial cell lineages [16]. F3 NSCs express the cell-type specific markers ATP-binding cassette G2 (ABCG2), Musashi-1 and nestin. The F3 cells were cultured as described previously [24]. The F3 cell line was infected with a replication-incompetent retroviral vector encoding β-galactosidase (*lacZ*) and puromycin-resistant genes and designated as F3.lacZ. The F3 cells were labelled with CellTracker CM-DiI (Invitrogen). Immediately before transplantation, the cells were incubated in 2 μM CellTracker solution for 5 min at 37 °C and for an additional 15 min at 4 °C. CM-DiI emits maximum fluorescence at 570 nm; labelled NSCs can be identified by fluorescence microscopy under which they appear red.

Firstly, we evaluated whether the DiI-labelled NSCs could migrate to the injured spinal cord in adult mice after intravenous transplantation. All surgeries were performed in 8-week-old female KSN mice (Japan SLC, Shizuoka, Japan) according to the protocols approved by an animal care and use committee at our institution. Spinal cord injury (SCI) at the T8 level was induced in accordance with the moderate weight compression method [9]. Briefly, under a surgical microscope, after a laminectomy was performed, the spinal cord was compressed by placing a 10 g-weighted 2 mm × 1 mm rectangular plastic plate on the dura mater for 5 min. The Basso, Beattie and Bresnahan (BBB) test was performed to evaluate the hind-limb locomotor function in an open field [4]. All injured animals showed a mean BBB score of 5, indicating slight movement of two joints and extensive movement of the third at 1 day after SCI; spontaneous improvement to an approximate score of 17 was subsequently observed. This SCI model produces a reproducible functional deficit that correlated with the histological findings. At 7 days after the induction of compressive injury, the injured ($n = 7$) and uninjured ($n = 7$) animals were injected intravenously via the tail vein with 1×10^7 DiI-labelled F3.lacZ cells diluted in 100 μL of 0.1 M phosphate-buffered saline (PBS). The control injured animals ($n = 7$) were injected with PBS alone. Seven days after NSC transplantation, the animals were euthanised and transcardially perfused with 4% paraformaldehyde (PFA). The removed spinal cords were fixed further in 4% PFA overnight at 4 °C. The tissues were cryoprotected by serial transfer through solutions of 10%, 15% and 20% sucrose in 0.1 M PBS. Using a cryostat, 16-μm-thick transverse serial sections were cut and stained with hematoxylin/eosin (H/E) or a solution containing 1 mg/mL X-gal, 5 mM $K_3Fe(CN)_6$, 5 mM $K_4Fe(CN)_6$ and 2 mM $MgCl_2$ in PBS. H/E staining of the representative sections of the spinal cord (Fig. 1A and B) indicated that the normal structure of the spinal cord parenchyma was destroyed, and a number of inflammatory cells had infiltrated the lesion. Donor X-gal$^+$ cells were observed to be extensively distributed in the contused area (Fig. 1C). Fluorescence microscopy revealed a large number of DiI-labelled cells in the lesion (Fig. 1D). All the NSCs

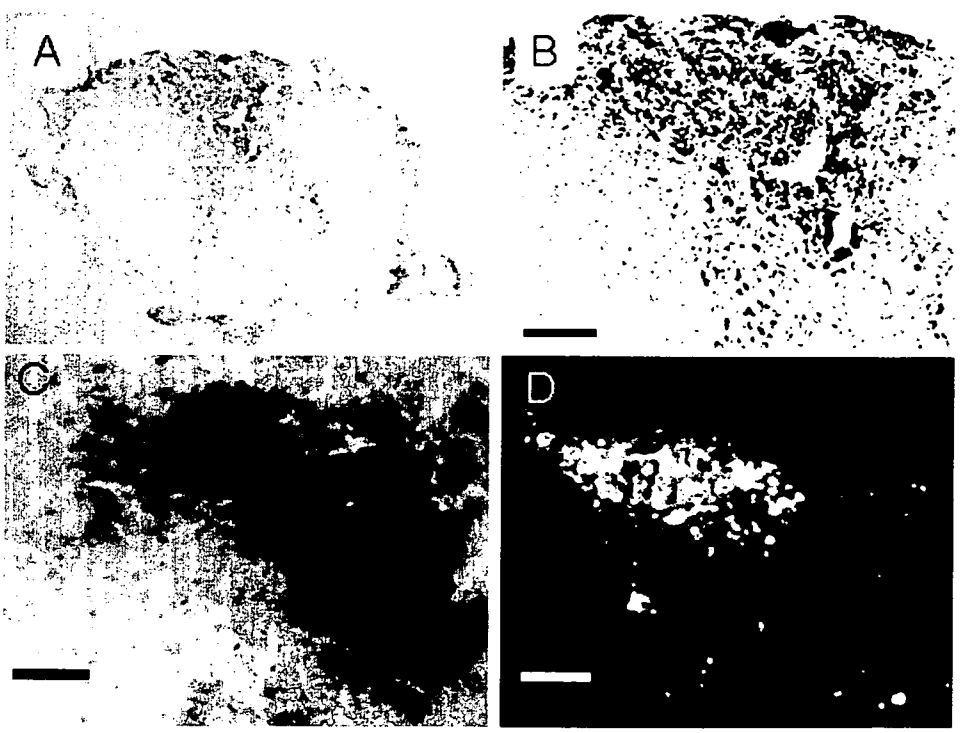

Fig. 1. (A) A representative hematoxylin/eosin-stained transverse section of the injured spinal cord 7 days after NSC transplantation; (B) high magnification of the boxed area in panel A; (C) X-gal-stained transverse section of the injured spinal cord 7 days after NSC transplantation; (D) observation by fluorescence microscopy at 570 nm. Scale bar: (B–D) 100 μm.

were located in or around the injured parenchyma; no cells were observed on the ventral, caudal or rostral sides of the injured sites, indicating that the migratory phenomenon exhibited some specificity. Conversely, in the control uninjured animals injected with F3.lacZ cells or in the injured animals injected with PBS, no DiI-labelled or X-gal$^+$ cells were observed in the spinal cord (data not shown). These findings suggest that the intravenously transplanted F3 cells can migrate diffusely to the injured spinal cord.

Secondly, to investigate the optimal timing of NSC transplantation, the injured animals ($n = 8$) were injected intravenously with 1×10^7 DiI-labelled F3.lacZ cells at 3, 7 or 10 days after the spinal cord injury. Seven days after F3 cell transplantation, the spinal cords were removed, and transverse sections were counterstained with the DNA-binding fluorochrome Hoechst 33342 for 30 min at room temperature in the dark. The sections were mounted in a fluorescent mounting medium (DakoCytomation, Glostrup, Denmark) and observed under a fluorescence microscope. The number of DiI-labelled cells was counted at the lesion site in a 0.25 mm^2 grid in every third serial section. The DiI-labelled NSCs that were transplanted at 3 days after the injury migrated to the lesion site at 46 ± 6 cells/mm^2 (Fig. 2A and D). When injected 7 days after the injury, a greater number of grafted cells (140 ± 10 cells/mm^2) were observed (Fig. 2B and D). However, only a few grafted cells (6 ± 2 cells/mm^2) were observed at the lesion site when human NSCs were injected at 10 days after the compression (Fig. 2C and D). Additionally, a number of DiI-labelled grafted cells were trapped in the lung, liver and spleen at 3 days after injection (Fig. 2E–G). Collectively, the observations indicated that NSC migration to the lesioned spinal cord was highest at 7 days and subsequently decreased. This finding prompted us to define the crosstalk between the injured spinal cord and NSCs; we thus investigated lesion-secreting chemo-attractants – stromal-derived factor (SDF)-1, hepatocyte growth factor (HGF), C3a and leukaemia inhibitory factor (LIF) – that could potentially regulate NSC trafficking.

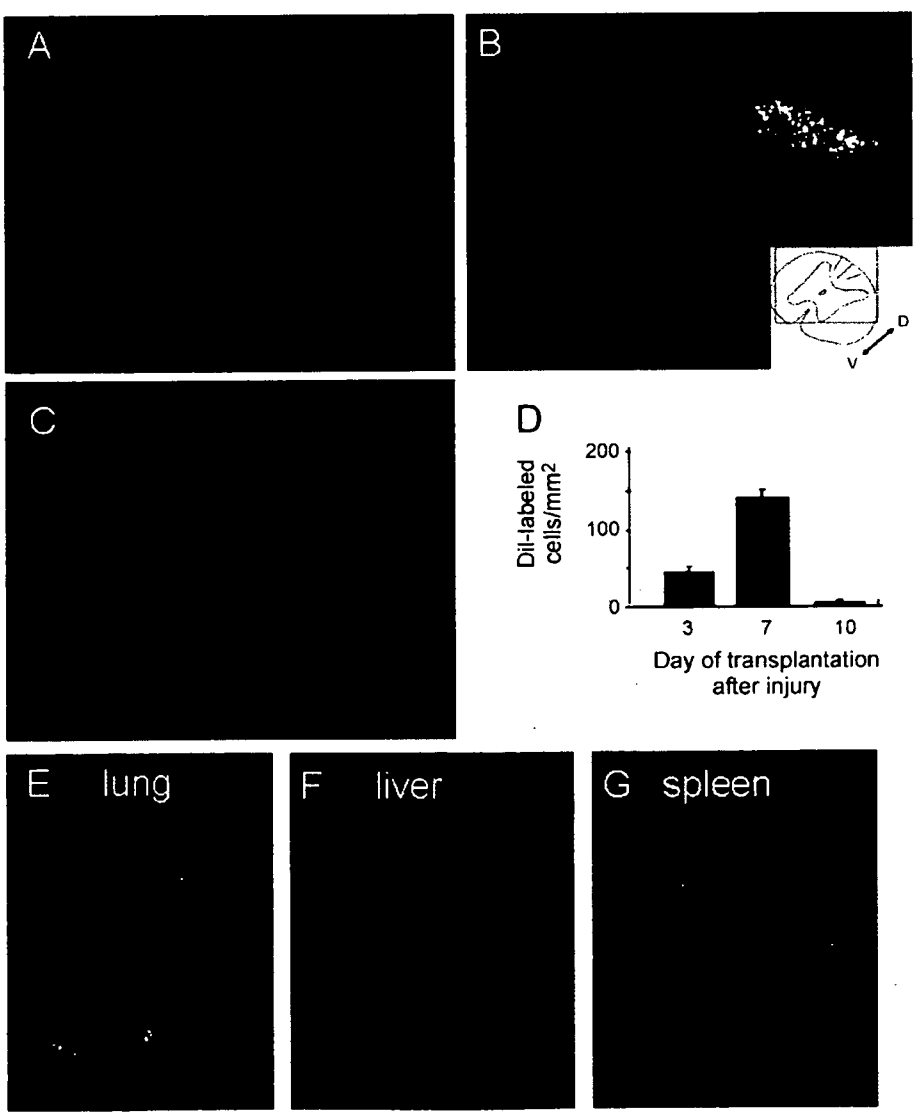

Fig. 2. The injured animals were injected intravenously with 1×10^7 DiI-labelled F3.lacZ cells at 3 (A), 7 (B) or 10 (C) days after spinal cord injury. (D) The number of DiI-labelled cells at the lesion site. Additionally, a number of DiI-labelled grafted cells were trapped in the lung (E), liver (F) and spleen (G) at 3 days after injection.

(A)

Gene	Sense	Antisense
SDF-1	5'-CGTGAGGCCAGGGAAGAGT-3'	5'-TGATGAGCATGGTGGGTTGA-3'
C3	5'-CCAGCCGGGGACCTCACTTGTAG-3'	5'-GGTCTTCCTGCCGTTTCTCTGTTG-3'
HGF	5'-CCAGATCCTTGTGGCTCCTATC-3'	5'-GGTTAGCGATTCAGTTCCGTG-3'
LIF	5'-TTCCCATCACCCCTGTAAATG-3'	5'-TTGGAGTACTTGGTCTAGTTCTTAG-3'
β2-microglobulin	5'-CATACGCCTGCAGAGTTAAGCA-3'	5'-GATCACATGTCTCGATCCCAGTAG-3'

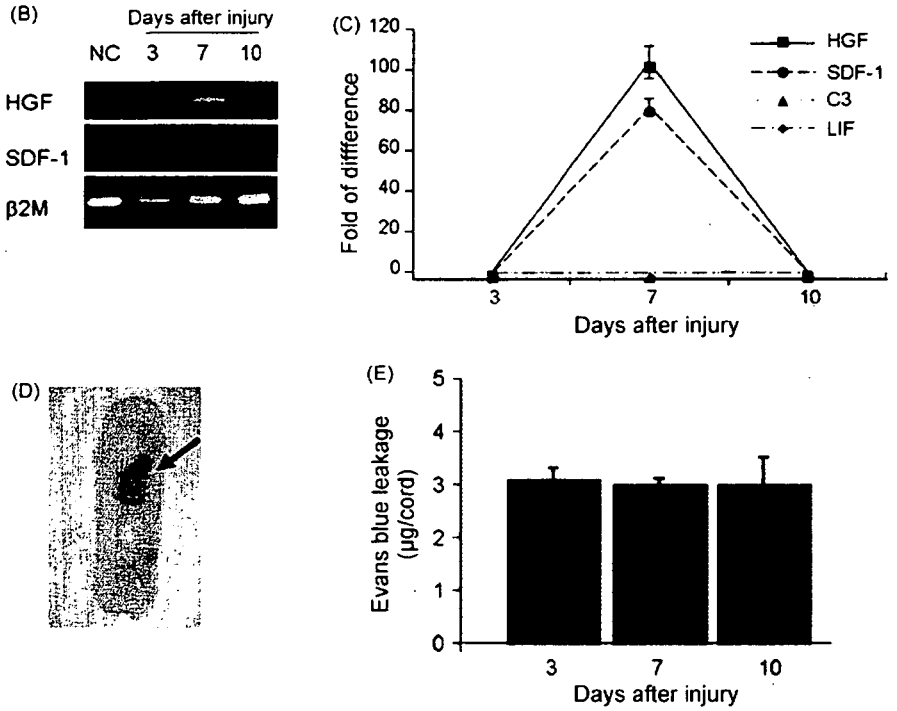

Fig. 3. (A) The primer sequences used in reverse transcription (RT)-polymerase chain reaction (PCR) and quantitative real-time RT-PCR. (B) RT-PCR. β_2-Microglobulin was used as an internal control. (C) Quantitative real-time RT-PCR. After being normalised by β_2-microglobulin expression, values are expressed as fold-changes compared to the control normal spinal cord. (D) A representative photograph of Evans blue extravasation in the lesion. (E) Quantitative assay of Evans blue leakage at 3, 7 and 10 days after injury.

Cytokines and chemokines secreted by altered tissues are crucial in directing the mobilization, circulation and homing of stem cells to the injured organs or cancerous tissues [17]. SDF-1 may play a central role in the homing process. F3 NSC cells have recently been reported to express CXCR4 – the receptor for SDF-1 – on their surfaces [15]. We have demonstrated that the HGF secreted by brain tumour cells is involved in the brain tumour tropism of NSCs [24]. Haematopoietic stem cells express a functional complement C3a receptor, and the C3aR–C3a axis plays a role in stem cell recruitment by enhancing the response of the stem cells to SDF-1 [23]. Similarly, LIF expression is up-regulated in an infarcted myocardium and induces the regeneration of the myocardium [26]. Therefore, a local increase in the expression of these chemokines and cytokines may enable the recruitment of NSCs to the lesioned spinal cord; this increase was examined in the lesion site 3, 7 and 10 days after injury by reverse transcription (RT)-PCR and quantitative real-time RT-PCR. The lesion site was dissected from the spinal cord under a microscope, and total RNA extracted using the TRIzol kit (Invitrogen) was subjected to DNase (Invitrogen) treatment prior to RT that was performed using the Transcriptor First Strand cDNA Synthesis Kit (Roche, Mannheim, Germany), according to the manufacturer's protocol. PCR amplification was performed using GoTaq DNA polymerase (Promega, Madison, WI) and the primers listed in Fig. 3A. The primers were designed using the Primer Express software. The PCR products were loaded on a 3% agarose gel and stained with ethidium bromide (Fig. 3B). Quantitative mRNA levels were detected by the LightCycler real-time RT-PCR system (Version 3.39) using the LightCycler FastStart DNA Master SYBR Green I (Roche). The primers listed in Fig. 3A were also used. The threshold cycle (Ct), i.e. the cycle number at which the amount of the amplified gene of interest reaches a fixed threshold, was subsequently determined. The relative quantification of SDF-1, C3, HGF and LIF mRNA expression was calculated by the comparative Ct method. The relative quantification value of the target normalised to an endogenous control β_2-microglobulin gene and relative to a calibrator is expressed as $2^{-\Delta\Delta Ct}$ (fold difference), where ΔCt = (the Ct of the target genes) – (the Ct of the β_2-microglobulin gene) and $\Delta\Delta Ct$ = (the ΔCt of the samples for the target genes) – (the ΔCt of the calibrator for the target genes). A dramatic expression of SDF-1 and HGF was observed in the day 7 SCI but not in the day 3 and day 10 SCI (Fig. 3B). C3a and LIF were not observed at any of the time points. The quantitative measurements revealed the expression levels of SDF-1 and HGF to be 101 ± 12-fold and 78 ± 3-fold of their respective values in

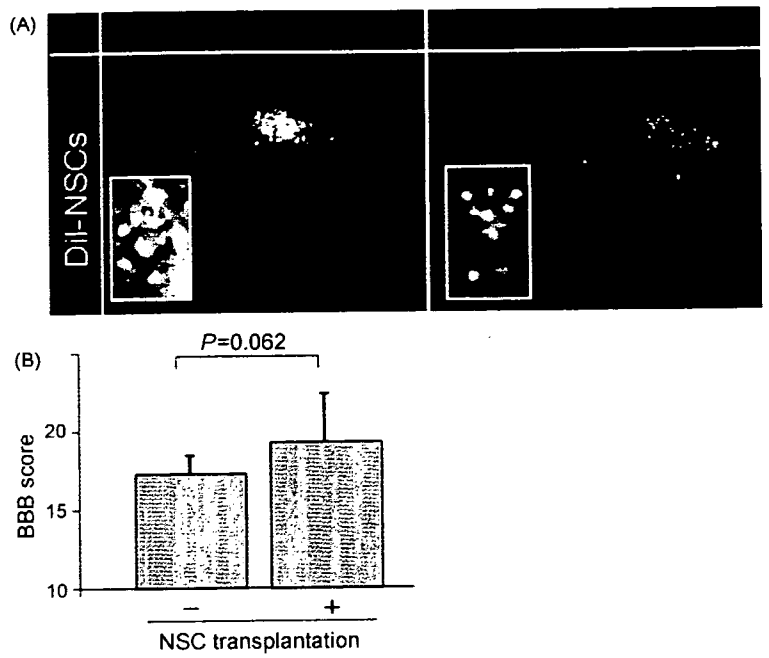

Fig. 4. (A) In vivo differentiation of the migrated NSCs in the lesioned spinal cord at 21 days. Merged images exhibiting DiI (red) and immunofluorescence (green) are shown. Sister sections visualised at high power. (B) The Basso, Beattie and Bresnahan (BBB) hind-limb locomotor function test at 21 days in animals treated with NSCs and control injured animals.

the control normal spinal cord (Fig. 3C). Next, in order to examine whether the SDF-1 and HGF expression that was the highest at 7 days was correlated with the time course of the disruption of the blood–brain barrier, quantitative Evans blue analysis was performed as described previously [8]. In brief, injured mice were injected intraperitoneally with 50 μg/g Evans blue dye in PBS at 3, 7 and 10 days after injury; 24 h after injection, the mice were perfused with PBS. The injured spinal cord was dissected. Evans blue extravasation was detected in the dorsal side of the lesioned cord (Fig. 3D). The dissected spinal cord was then homogenised in 0.5 mL of 50% trichloroacetic acid. The sample was centrifuged at 13,000 rpm for 10 min. The supernatant was collected and diluted in 100% ethanol in a 1:4 ratio, and absorbance (620 nm) was measured using an ELISA plate reader. These values are plotted on a graph as the amount of Evans blue leakage (μg)/spinal cord (Fig. 3E). There was no change in Evans blue leakage (approximately 3 μg) among any time points, indicating that the blood–brain barrier was disrupted by the third day after injury and its time course was minimally correlated with that of SDF-1 and HGF expression from the lesion.

Finally, to investigate the in vivo differentiation of the migrated NSCs and neurobehavioural recovery, the injured animals ($n = 8$) were injected intravenously with 1×10^7 DiI-labelled F3.lacZ cells at 7 days after injury. Twenty-one days after NSC transplantation, the BBB test was performed by observers blinded to the experimental groups, and the spinal cords were removed and subjected to immunohistochemistry with primary antibodies (Abs): mouse anti-neuron-specific class III beta-tubulin Ab (1:50; Genzyme-Techne, Minneapolis, MN) and rabbit anti-glial fibrillary acidic protein (GFAP) Ab (1:100; DakoCytomation), followed by the relevant Alexa Fluor 488-conjugated-secondary Abs. GFAP-immunoreactive (IR) and beta III-tubulin–IR NSCs labelled with DiI were found intermixed in the lesioned spinal cord; the ratio of the GFAP–IR NSCs to the beta III-tubulin–IR NSCs was approximately 3:2 (Fig. 4A). This finding suggests that during the first 3 weeks, the NSCs underwent differentiation, which is consistent with the results of previous reports [6,10]. Once transplanted into the spinal cord, NSCs adapt to the region of engraftment by differentiating into the appropriate neuronal and glial subpopulations. At the end of the first 3 weeks, we observed a tendency of remarkable functional recovery in animals treated with NSCs compared to control injured animals although it was not statistically significant ($p = 0.062$, two-tailed Student's t-test) (Fig. 4B). Human NSCs have recently been demonstrated to express significant amounts of nerve growth factor and brain-derived neurotrophic factors and facilitate functional recovery in the stroke model [18]. Thus, the differentiated NSCs in the lesioned spinal cord that we observed may eventually restore neurological function.

Our principal finding is that intravenously transplanted human NSCs migrate preferentially to the injured spinal cord and differentiate into neuronal and glial subpopulations. Consistent with a previous report [11], we observed a substantial number of injected NSCs in the lesion site of the spinal cord. Moreover, Willing et al. have demonstrated that the intravenous delivery of NSCs might be more effective than their striatal delivery in producing long-term functional benefits to animals suffering from stroke [25]. This finding supported our results demonstrating glial and neuronal differentiation of NSCs, indicating that the intravenous NSC injection activates the microenvironment of the injured spinal cord to stimulate self-regeneration. Further, the migration of the transplanted NSCs to the lesioned spinal cord was highest at day 7 after injury,

correlating with the peak of HGF and SDF-1 mRNA expression in the lesion. Recently, we demonstrated that HGF is an important chemo-attractant for NSCs to brain tumours by using the migration assay blocked with a neutralizing monoclonal antibody [24]. These findings may vary following the disruption of the blood–brain barrier or the number of inflammatory cells that infiltrated the lesion. In this study, we demonstrated that the blood–brain barrier was disrupted as early as the third day after injury. Additionally, we have previously demonstrated that inflammatory leukocytes infiltrate lesions by 24 h following injury, as measured by myeloperoxidase activity [12]. These findings suggest that NSCs migrate actively, but not passively, and this is accompanied by extensive crosstalk between lesions and NSCs. The transplantation of renewable, homogeneous, multi-potent and well-characterised NSCs into the damaged neural tissues should enable the replacement of lost cells and restore the damaged functions. We have demonstrated that the intravenous injection of human NSCs is a promising tool that can be employed as a renewable source for replacing lost cells or for delivering therapeutic genes for the treatment of spinal cord injury.

ISSN 0304-3940 (print)

References

[1] K.S. Aboody, A. Brown, N.G. Rainov, K.A. Bower, S. Liu, W. Yang, J.E. Small, U. Herrlinger, V. Ourednik, P.M. Black, X.O. Breakefield, E.Y. Snyder, Neural stem cells display extensive tropism for pathology in adult brain: evidence from intracranial gliomas, Proc. Natl. Acad. Sci. U.S.A. 97 (2000) 12846–12851.

[2] S. Akiyama, O. Honmou, T. Kato, T. Uede, K. Hashi, J.D. Kocsis, Transplantation of clonal neural precursor cells derived from adult human brain establishes functional peripheral myelin in the rat spinal cord, Exp. Neurol. 167 (2001) 27–39.

[3] A. Bakshi, C. Hunter, S. Swanger, A. Lepore, I. Fischer, Minimally invasive delivery of stem cells for spinal cord injury: advantages of the lumbar puncture technique, J. Neurosurg. Spine 1 (2004) 330–337.

[4] D.M. Basso, M.S. Beattie, J.C. Bresnahan, A sensitive and reliable locomotor rating scale for open field testing in rats, J. Neurotrauma 12 (1995) 1–21.

[5] A.B. Brown, W. Yang, N.O. Schmidt, R. Carroll, K.K. Leishear, N.G. Rainov, P.M. Black, X.O. Breakefield, K.S. Aboody, Intravascular delivery of neural stem cell lines to target intracranial and extracranial tumors of neural and non-neural origin, Hum. Gene Ther. 14 (2003) 1777–1785.

[6] K. Chu, M. Kim, S.W. Jeong, S.U. Kim, B.W. Yoon, Human neural stem cells can migrate, differentiate, and integrate after intravenous transplantation in adult rats with transient forebrain ischemia, Neurosci. Lett. 343 (2003) 129–133.

[7] P.V. Dickson, J.B. Hamner, R.A. Burger, E. Garcia, A.A. Ouma, S.U. Kim, C.Y. Ng, J.T. Gray, K.S. Aboody, M.K. Danks, A.M. Davidoff, Intravascular administration of tumor tropic neural progenitor cells permits targeted delivery of interferon-beta and restricts tumor growth in a murine model of disseminated neuroblastoma, J. Pediatr. Surg. 42 (2007) 48–53.

[8] D.L. Dickstein, K.E. Biron, M. Ujiie, C.G. Pfeifer, A.R. Jeffries, W.A. Jefferies, A beta peptide immunization restores blood–brain barrier integrity in Alzheimer disease, FASEB J. 20 (2006) 426–433.

[9] M. Farooque, Spinal cord compression injury in the mouse: presentation of a model including assessment of motor dysfunction, Acta Neuropathol. (Berl.) 100 (2000) 13–22.

[10] J.D. Flax, S. Aurora, C. Yang, C. Simonin, A.M. Wills, L.L. Billinghurst, M. Jendoubi, R.L. Sidman, J.H. Wolfe, S.U. Kim, E.Y. Snyder, Engraftable human neural stem cells respond to developmental cues, replace neurons, and express foreign genes, Nat. Biotechnol. 16 (1998) 1033–1039.

[11] Y. Fujiwara, N. Tanaka, O. Ishida, Y. Fujimoto, T. Murakami, H. Kajihara, Y. Yasunaga, M. Ochi, Intravenously injected neural progenitor cells of transgenic rats can migrate to the injured spinal cord and differentiate into neurons, astrocytes and oligodendrocytes, Neurosci. Lett. 366 (2004) 287–291.

[12] M. Hara, M. Takayasu, K. Watanabe, A. Noda, T. Takagi, Y. Suzuki, J. Yoshida, Protein kinase inhibition by fasudil hydrochloride promotes neurological recovery after spinal cord injury in rats, J. Neurosurg. 93 (2000) 94–101.

[13] K. Ichihara, T. Taguchi, Y. Shimada, I. Sakuramoto, S. Kawano, S. Kawai, Gray matter of the bovine cervical spinal cord is mechanically more rigid and fragile than the white matter, J. Neurotrauma 18 (2001) 361–367.

[14] S.W. Jeong, K. Chu, K.H. Jung, S.U. Kim, M. Kim, J.K. Roh, Human neural stem cell transplantation promotes functional recovery in rats with experimental intracerebral hemorrhage, Stroke 34 (2003) 2258–2263.

[15] S.K. Kim, S.U. Kim, I.H. Park, J.H. Bang, K.S. Aboody, K.C. Wang, B.K. Cho, M. Kim, L.G. Menon, P.M. Black, R.S. Carroll, Human neural stem cells target experimental intracranial medulloblastoma and deliver a therapeutic gene leading to tumor regression, Clin. Cancer Res. 12 (2006) 5550–5556.

[16] S.U. Kim, Human neural stem cells genetically modified for brain repair in neurological disorders, Neuropathology 24 (2004) 159–171.

[17] O. Kollet, S. Shivtiel, Y.Q. Chen, J. Suriawinata, S.N. Thung, M.D. Dabeva, J. Kahn, A. Spiegel, A. Dar, S. Samira, P. Goichberg, A. Kalinkovich, F. Arenzana-Seisdedos, A. Nagler, I. Hardan, M. Revel, D.A. Shafritz, T. Lapidot, HGF, SDF-1, and MMP-9 are involved in stress-induced human CD34+ stem cell recruitment to the liver, J. Clin. Invest. 112 (2003) 160–169.

[18] H.J. Lee, K.S. Kim, E.J. Kim, H.B. Choi, K.H. Lee, I.H. Park, Y. Ko, S.W. Jeong, S.U. Kim, Brain transplantation of immortalized human neural stem cells promotes functional recovery in mouse intracerebral hemorrhage stroke model, Stem Cells 25 (2007) 1204–1212.

[19] Y. Ogawa, K. Sawamoto, T. Miyata, S. Miyao, M. Watanabe, M. Nakamura, B.S. Bregman, M. Koike, Y. Uchiyama, Y. Toyama, H. Okano, Transplantation of in vitro-expanded fetal neural progenitor cells results in neurogenesis and functional recovery after spinal cord contusion injury in adult rats, J. Neurosci. Res. 69 (2002) 925–933.

[20] H. Okano, Y. Ogawa, M. Nakamura, S. Kaneko, A. Iwanami, Y. Toyama, Transplantation of neural stem cells into the spinal cord after injury, Semin. Cell Dev. Biol. 14 (2003) 191–198.

[21] J. Ourednik, V. Ourednik, W.P. Lynch, M. Schachner, E.Y. Snyder, Neural stem cells display an inherent mechanism for rescuing dysfunctional neurons, Nat. Biotechnol. 20 (2002) 1103–1110.

[22] K.I. Park, S. Liu, J.D. Flax, S. Nissim, P.E. Stieg, E.Y. Snyder, Transplantation of neural progenitor and stem cells: developmental insights may suggest new therapies for spinal cord and other CNS dysfunction, J. Neurotrauma 16 (1999) 675–687.

[23] J. Ratajczak, R. Reca, M. Kucia, M. Majka, D.J. Allendorf, J.T. Baran, A. Janowska-Wieczorek, R.A. Wetsel, G.D. Ross, M.Z. Ratajczak, Mobilization studies in mice deficient in either C3 or C3a receptor (C3aR) reveal a novel role for complement in retention of hematopoietic stem/progenitor cells in bone marrow, Blood 103 (2004) 2071–2078.

[24] S. Shimato, A. Natsume, H. Takeuchi, T. Wakabayashi, M. Fujii, M. Ito, S. Ito, I.H. Park, J.H. Bang, S.U. Kim, J. Yoshida, Human neural stem cells target and deliver therapeutic gene to experimental leptomeningeal medulloblastoma, Gene Ther. 14 (2007) 1132–1142.

[25] A.E. Willing, J. Lixian, M. Milliken, S. Poulos, T. Zigova, S. Song, C. Hart, J. Sanchez-Ramos, P.R. Sanberg, Intravenous versus intrastriatal cord blood administration in a rodent model of stroke, J. Neurosci. Res. 73 (2003) 296–307.

[26] Y. Zou, H. Takano, M. Mizukami, H. Akazawa, Y. Qin, H. Toko, M. Sakamoto, T. Minamino, T. Nagai, I. Komuro, Leukemia inhibitory factor enhances survival of cardiomyocytes and induces regeneration of myocardium after myocardial infarction, Circulation 108 (2003) 748–753.

J Neurooncol
DOI 10.1007/s11060-007-9335-1

LAB INVESTIGATION — HUMAN/ANIMAL TISSUE

Inhibition of Aurora-B function increases formation of multinucleated cells in *p53* gene deficient cells and enhances anti-tumor effect of temozolomide in human glioma cells

Takaya Tsuno · Atsushi Natsume · Shun Katsumata · Masaaki Mizuno · Mitsugu Fujita · Hirokatsu Osawa · Norimoto Nakahara · Toshihiko Wakabayashi · Yu-ichiro Satoh · Masaki Inagaki · Jun Yoshida

Received: 22 December 2006 / Accepted: 16 January 2007

Abstract Cell division is an elemental process, and mainly consists of chromosome segregation and subsequent cytokinesis. Some errors in this process have the possibility of leading to carcinogenesis. Aurora-B is known as a chromosomal passenger protein that regulates cell division. In our previous studies of giant cell glioblastoma, we reported that multinucleated giant cells resulted from aberrations in cytokinesis with intact nuclear division occurring in the early mitotic phase, probably due to Aurora-B dysfunction. In this study, as we determined *p53* gene mutation occurring in multinucleated giant cell glioblastoma, we investigated the role of Aurora-B in formation of multinucleated cells in human neoplasm cells with various p53 statuses as well as cytotoxity of glioma cells to temozolomide (TMZ), a common oral alkylating agent used in the treatment of gliomas. The inhibition of Aurora-B function by small-interfering (si)RNA led to an increase in the number of multinucleated cells and the ratios of G2/M phase in p53-mutant and p53-null cells, but not in p53-wild cells or the cells transduced adenovirally with wild-p53. The combination of TMZ and Aurora-B-siRNA remarkably inhibited the cell viability of TMZ-resistant glioma cells. Accordingly, our results suggested that Aurora-B dysfunction increases in the appearance of multinucleated cells in *p53* gene deficient cells, and TMZ treatment in combination with the inhibition of Aurora-B function may become a potential therapy against *p53* gene deficient and chemotherapeutic-resistant human gliomas.

Keywords Aurora-B · siRNA · Temozolomide · Glioma · Multinucleated cells · p53

T. Tsuno · A. Natsume · S. Katsumata · M. Mizuno · M. Fujita · H. Osawa · N. Nakahara · T. Wakabayashi · Y. Satoh · J. Yoshida (✉)
Department of Neurosurgery, Nagoya University Graduate School of Medicine, 65 Tsurumai-cho, Showa-ku, Nagoya, Aichi 466-8550, Japan
e-mail: jyoshida@med.nagoya-u.ac.jp

A. Natsume · T. Wakabayashi · J. Yoshida
Center for Genetic and Regenerative Medicine, Nagoya University Hospital, Nagoya, Aichi, Japan

M. Inagaki
Division of Biochemistry, Aichi Cancer Center Research Institute, Nagoya, Aichi, Japan

Introduction

Cell division plays a fundamental role in bequeathing accurate genetic information to daughter cells. Malignant neoplastic cells are considered as being unable to regulate cell division due to genetic alterations. Point mutation, deletion, translocation, and amplification are known genetic changes in those cells, and many of those cells also have an abnormal number of chromosomes [1, 2]. It is proposed that the abnormality of chromosome segregation causes aneuploidy, resulting in oncogenesis [3]. These abnormalities are associated with many molecules such as CDK (Cyclin-dependent kinase)/Cyclin, PLK (Polo-like kinase), and Aurora-related kinases.

The Aurora kinase family is preserved in the eukaryote, and is recognized as participating in chromosome segregation and cell division by analyses using small-interfering (si)RNA and mutants in budding and fission yeast, drosophila, and *C. elegans* [4, 5]. Humans and mice have three kinds of aurora kinases referred to

as Aurora-A, B, and C; both Aurora-A and -B are overexpressed in tumor cells, and the peak of activation of Aurora-A is observed earlier than that of Aurora-B during the cell cycle, including mitotic phase which is composed of prophase, prometaphase, metaphase, anaphase, telophase, and cytokinesis [6]. Aurora-A is principally associated with prophase through telophase, and is related to centrosome maturation and spindle assembly. [4, 6–10] On the other hand, Aurora-B has been considered to localize in the chromosomes during the early mitotic phase and move to the midbody during anaphase, and then produce postmitotic bridges during telophase [4–6, 11]. As Aurora-B shows its migration during the mitotic phase, it is referred to as a chromosomal passenger protein [12]. The *Aurora-B* gene localizes in the human chromosome 17p13.1 in which the incidence of genomic imbalance and loss of heterozygosity (LOH) has been detected in many cancers [13, 14]. Overexpressions of mRNA and protein of Aurora-B are often detected in some human cancer cells [15]. Aurora-C is the most unknown kinase of these Aurora kinases. It has been reported that higher expression levels of Aurora-C in several cancer cell lines were observed than in normal fibroblasts. Aurora-C is localized in the centrosome during mitosis from anaphase to cytokinesis, and may play a role in centrosome function at later stages of mitosis [16]. Thus, it is possible to assume that errors in chromosome segregation and cytokinesis in the mitotic phase result in aneuploidy which can lead to cell death or oncogenesis.

Giant cell glioblastoma is a rare variant of glioblastomas, and is characterized by predominance of large, bizarre, multinucleated giant cells [17]. It has been reported that this variant indicated a somewhat more favorable prognosis than typical glioblastomas [17–21]. Furthermore, large, multinucleated cells have been reported to be generally non-proliferating in proliferation studies of glioblastomas [18, 22]. We previously reported studies of the multinucleated giant cells in glioblastoma multiforme using site-specific phosphorylated anti-vimentin antibodies and anti-Aurora-B antibody [23, 24]. These studies indicated that multinucleated giant cells resulted from aberrations in cytokinesis with intact nuclear division occurring in the early mitotic phase, probably due to Aurora-B dysfunction.

In addition, this glioblastoma subtype contains a high frequency of p53 mutations [17, 18, 21]. It has been clear that mutations in this gene are demonstrated in more than 50% of human cancers, and in 29–48% of astrocytic tumors [25]. p53 plays an important role in response to genotoxic stress, such as DNA damage caused by radiation, drugs, and so on. DNA damage leads to cell cycle arrest in the G1 or G2 phase mediated by p53. Apoptosis can be also mediated by p53 to prevent inheritance of damaged gene information [26, 27]. Therefore, in the cells with mutant p53, the cell cycle arrest and apoptosis cannot be indicated effectively after exposure of DNA damage, followed by uncontrolled cell divisions and an increase in the number of the cells with abnormal chromosomes, such as multinucleated cells.

In the current study, we investigated whether the formation of multinucleated cells could be associated not only with dysfunction of Aurora-B but also with that of p53 using human glioma cells (mutant and wild type p53) as well as human osteosarcoma cells (p53-null). As a result, Aurora-B dysfunction induced multinucleated cells more significantly in tumor cells with mutant- or null-p53 than with wild-p53. In addition, we further examined whether such a multinucleated cell-induction by Aurora-B inactivation enhanced chemosensitivity to an alkylating agent, temozolomide (TMZ), in glioma cells with or without functional p53.

Materials and methods

Cell culture

Human glioma cell lines (U251MG, T98G, and U87MG) were derived from the Memorial Sloan-Kettering Cancer Institute (New York, NY), and human osteosarcoma cell line (Saos-2) were purchased from American Type Culture Collection (Manassas, VA). The cells were maintained at 37°C in a humidified atmosphere of 5% CO_2 in air. U251MG and T98G cells were maintained in Eagle's medium, U87MG cells in RPMI Medium 1640, and Saos-2 in Dulbecco's Modified Eagle Medium (Nissui, Tokyo, Japan), respectively. These media were supplemented with 10% fetal bovine serum (FBS), 5 mM L-glutamine, 2 mM nonessential amino acids, and antibiotics (100 U/ml penicillin and 100 μg/ml streptomycin). It has been reported that U251MG and T98G cells have a mutant type and nonfunctioning p53, U87MG cells have wild type p53, and Saos-2 cells show p53-null [28–30].

Reagents and antibodies

TMZ were kindly supplied by the Schering-Plough Research Institute (Kenilworth, NJ). The following primary antibodies were used: mouse anti-Aurora-B monoclonal antibody (αAIM-1; BD Biosciences, San Jose, CA), mouse anti-p53 monoclonal antibody

(DO-1; Santa Cruz Biotechnology, Inc, Santa Cruz, CA), and rabbit anti-actin polyclonal antibody (Sigma-Aldrich, St. Louis, MO). The secondary antibodies used were horseradish peroxidase (HRP)-conjugated anti-mouse or anti-rabbit IgG (Santa Cruz Biotechnology).

Design of siRNAs

The target region in the human Aurora-B complementary DNA (cDNA) is 5′-AAGGTGATGGAGAATAGCAGT-3′, as described previously [31]. The target sequence of non-silencing cDNA is 5′-AATTCTCCGAACGTGTCACGT-3′. (The cells in which this non-silencing was transfected were used as a control in this study.) These synthetic sense and antisense oligonucleotides were obtained from QIAGEN GmbH (Hilden, Germany). For the annealing of siRNA oligos, sense and antisense oligonucleotides were incubated in siRNA Suspension Buffer (QIAGEN GmbH) for 1 min at 90°C, followed by 60 min at 37°C. The day before transfection, 1×10^5 trypsinized cells were plated in each well of 6-well plates. After 24 h, siRNA oligos were mixed with Oligofectamine Reagent (Invitrogen, Carlsbad, CA) in OPTI-MEM medium (Invitrogen). Cultured cells were washed with medium without serum and added to the siRNA-oligofectamine mixture, of which the final concentration was 200 nM. The medium containing 10% FBS was replaced 4 h later.

Adenoviral vectors

AxCAZ2-F/K20 and AxCAhp53-F/K20 were used. The former is an adenoviral vector possessing the *LacZ* gene as a reporter and the latter is also an adenoviral vector expressing the human *p53* gene. Both were kindly provided by H. Hamada, Sapporo Medical University, Sapporo, Japan [32]. These vectors were condensed for five days twice using 293 cells, followed by being transduced into U251MG, T98G, and Saos-2 cells for 24 h. The amount of virus was necessary for the cells to be infected completely.

Molecular genetic analysis of giant cell glioblastomas

Tumor and blood samples were obtained from three patients with giant cell glioblastoma treated at the Nagoya University Hospital, Nagoya, Japan. All tumors were classified and graded according to the guidelines of the Would Health Organization (WHO). Previously, all of their paraffin-embedded sections were immunostained with site-specific phosphorylated anti-vimentin antibodies (4A4, YT33, TM71, HTA28, and YG72) and anti-Aurora-B antibody (αAIM-1), and determined as harboring Aurora-B dysfunction [23]. Genomic DNA from leukocytes and tumor tissues was extracted by standard methods. LOH assay and *p53* sequencing were performed using ABI PRISM 310 Genetic Analyzer (Applied Biosystems, Foster City, CA). For the LOH assay, the following microsatellite markers that are located at the most frequently deleted sites in gliomas were used: D1S244, D1S199, and D1S2734 for 1p (1p36); D19S219, D19S412, and D19S112 for 19q (19q13); and D10S1744, D10S583, and D10S1680 for 10q (10q22–23). The primer sequences for these markers are available from the Genome Database. The DNA extracted from each patient's blood was used as the normal control and compared with the tumor DNA. In such setting, if at least one of the three markers is informative, it can distinguish LOH cases from non-LOH ones. The LOH result was considered positive if the allelic signal intensity of the tumor sample was reduced by >50% compared to the corresponding allele in the patient's control DNA. For direct sequencing, exons 5–8 of *p53* were amplified with the previously published primer pairs [33] and directly sequenced using the BigDye Terminator Sequencing Kit (Applied Biosystems). We repeated the LOH and p53 mutation analyses twice. DNA methylation patterns in the promoter region of the *MGMT* gene (O^6-methylguanine-DNA methyltransferase: GenBank accession no. X_61657) were determined by methylation-specific polymerase chain reaction (PCR), as previously described [34]. All PCRs were performed with positive controls for unmethylated and methylated alleles and negative water control. Human placental DNA was treated in vitro with excess SssI methyltransferase (New England Biolabs, Ipswich, MA), thereby generating DNA that was completely methylated at the CpG sites; this methylated DNA served as the positive control for the methylated *MGMT*. Each PCR product was loaded onto 3% agarose gel, stained with ethidium bromide, and visualized under UV illumination.

Western blot analysis

The cells were collected 48 h after transfection of siRNA, then lysed in cell lysis buffer (Cell Signaling Technology, Inc., Beverly, MA) with 1 mM phenylmethylsulfonyl fluoride, 10 μg/ml aprotinin, and 50 mM sodium fluoride. Solubilized cell constituents were centrifuged at 13000 × *g* for 10 min. Aliquots of

supernatant were assayed for protein content using Bio-Rad DC protein assay kit (Bio-Rad Laboratories, Hercules, CA). Protein samples were denatured in gel-loading buffer (New England Biolabs) for 5 min at 99°C. Equivalent amounts of protein were applied to each well of gel containing sodium dodecyl sulfate (SDS) and 12.5% (w/v) polyacrylamide (Bio-Rad Laboratories) for electrophoresis. Subsequently, these proteins were transferred to polyvinylidene difluoride membranes (Millipore, Billerica, MA) and blocked with blocking buffer (0.05 M Tris–HCl; pH 7.5, 0.15 M NaCl, 1% skim-milk in T-PBS consisting of phosphate-buffered saline (PBS) with 0.05% of Tween20). The membranes were then washed with T-PBS, and incubated with primary antibodies, followed by 1:3000 dilution of HRP-conjugated secondary antibodies. After several washings with T-PBS, proteins were detected using an enhanced chemiluminescence reagent (ECL Western Blotting Detection System: Amersham Biosciences Corp., Piscataway, NJ). Where appropriate, membranes were stripped with a solution containing 2% SDS, 62.5 mM Tris-HCl; pH 6.8, 0.7% β-mercaptoethanol for 20 min 50°C, washed several times with T-PBS, and then reblocked with blocking buffer before addition of another primary antibody.

Morphological study

Approximately 1×10^4 cells were plated on a micro cover glass (Matsunami Glass Industries Ltd., Osaka, Japan) in each well of 24-well plates, then transfected with siRNA as described above. The cells on the micro cover glasses were fixed with 4% paraformaldehyde and 0.1% Triton X-100 in PBS 48 h after transfection, and washed with PBS. For fluorescent labeling of nuclei, the cells were incubated with Hoechst 33342 (Sigma-Aldrich). After washing with PBS and distilled water, these micro cover glasses were mounted on glass slides over a drop of Fluorescent Mounting Medium (DakoCytomation California, Inc., Carpinteria, CA). These slides were examined under a Nikon Eclipse E600 microscope with a Plan Apo $20 \times /0.75$ oil immersion lens (Nikon Corp., Tokyo, Japan). The images were captured with Nikon ACT-1 software.

Flow cytometry (DNA histogram)

The cells were collected 48 h after transfection of siRNA, and fixed in 70% ethanol for 3 days at –20°C. These cells were washed with PBS, and resuspended in 250 µl of PBS with 1% RNase A (Roche Diagnostics, Indianapolis, IN) for 25 min at 37°C, subsequently stained in 25 µg/ml propidium iodine (PI) for 20 min at 4°C. Finally, the deoxyribonucleic acid (DNA) content was determined by flow cytometry (Coulter EPICS XL; Coulter Electronics, Hialeah, FL). The percentages of G2/M phase and multinucleated cells were analyzed and quantified by WinMDI 2.8 software.

Anti-tumor effect of TMZ and/or Aurora-B inhibition

Approximately 5×10^4 cells were plated in each well of 24-well plates, and transfected at the same ratio of siRNA as described above. Forty-eight hours after transfection, TMZ was added to the medium (for a final concentration of 100 µM). Cell viability was determined by the trypan-blue exclusion method on day 5, and each viability ratio (%) was demonstrated as [a subject of experiment]/[Control (non-silencing-siRNA)] $\times$ 100.

Statistical analysis

The differences in cell viability were calculated using Mann–Whitney *U*-test, and were considered to be significant if the probability value was less than 0.05.

Results

Molecular genetic analysis of giant cell glioblastomas

Giant cell glioblastoma is a curious clinicopathological variant of glioblastomas. Several studies have shown that this subtype is associated with a somewhat better prognosis than typical glioblastoma, and contains a higher frequency of p53 mutation. We retrieved three cases of giant cell glioblastoma from our clinical records; patients' ages at initial diagnosis ranged from 19 to 31 years old (median age, 26.3 years). All patients underwent surgical resection followed by nitrosourea-based chemotherapy and conventional radiotherapy (60 Gy). Their outcomes are listed in Table 1. Our previous study using site-specific phosphorylated antibodies indicated that multinucleated giant cells in those paraffin-embedded sections resulted from Aurora-B dysfunction. In this study, LOH status of chromosomes 1p/19q/10q, methylation of the MGMT promoter, and exons 5 to 8 of the *p53* gene for mutation were examined. None of the tumors showed 1p/19q/10q LOH and MGMT methylation, whereas p53 mutations were observed in all tumors tested.

Table 1 Molecular genetic findings and clinical data in giant cell glioblastomas

Patient	Age (years)	Surgery	CTx	RTx (Gy)	TTP (months)	OS (months)	LOH			MGMT	P53		
							1p	19q	10q		Exon	Codon	Mutation
1	19	Partial	IM	60	30	64	–	–	–	UM	8	273	CGT → TGT
2	31	Subtotal	IM	60	7	24	–	–	–	UM	5	164	AAG → GAG
3	29	Subtotal	IM	60	7	24	–	–	–	UM	8	273	CGT → GGT

CTx = initial chemotherapy; RTx = radiotherapy; TTP = time to progression; OS = overall survival
LOH = loss of heterozygosity; IM = interferon-beta and MCNU (ramunistine); UM = unmethylated

The expression of Aurora-B and p53 in human glioma cells and human osteosarcoma cells

We transfected siRNA into U251MG, T98G, U87MG, and Saos-2 cells to inhibit Aurora-B function, and evaluated the efficacy by western blot analysis. The results are shown in Fig. 1. The levels of Aurora-B expression were inhibited in all of the cell lines, but the levels of p53 expression did not change in the glioma cell lines. Overexpression of p53 was obtained 48 h after adenovirus-mediated transduction of *p53* gene into Saos-2 cells.

Morphological changes of human glioma cells and human osteosarcoma cells by inhibiting Aurora-B function with or without p53 gene transduction

To investigate the morphological changes of human glioma cells by inhibiting Aurora-B function, fluorescence microscopy was performed 48 h after transfection of Aurora-B-siRNA. Representative pictures are shown in Fig. 2a. Increases in the number of multinucleated cells were detected in Aurora-B-inhibited U251MG and T98G cells (mutant type p53), but not in Aurora-B-inhibited U87MG cells (wild type p53). In addition, we transfected Aurora-B-siRNA 24 h after transduction of AxCAZ2-F/K20 or AxCAhp53-F/K20 into

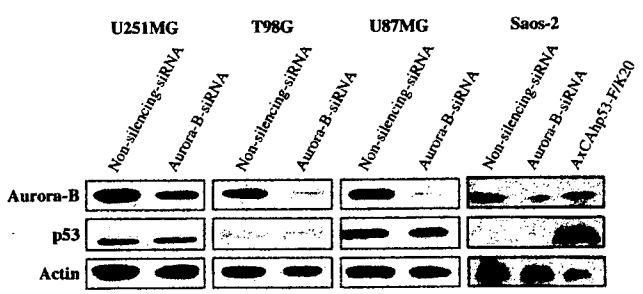

Fig. 1 Expressions of Aurora-B and p53. The expression levels of Aurora-B were inhibited 48 h after transfection of Aurora-B-siRNA into all of the cell lines. No change was detected at the levels of p53 expression in any of these glioma cell lines. The expression of p53 was induced 48 h after transduction of AxCAhp53-F/K20 into Saos-2 cells

U251MG and T98G cells. The representative pictures are shown in Fig. 2b. We observed a remarkable reduction in the number of multinucleated cells in the *p53* gene-transduced cells. To further investigate whether multinucleated cells by Aurora-B inhibition are associated with p53 status, we performed similar experiments in Saos-2 cell line that is p53-null. In Saos-2 cells, as well as U251MG and T98 cells (mutant type p53), the inhibition of Aurora-B function increased the number of multinucleated cells with failure of chromosome arrangement. On the other hand, in *p53* gene-transduced Saos-2 cells, no increase in the number of multinucleated cells was observed after Aurora-B inhibition (Fig. 2c).

Cell cycle analysis

To confirm our morphological observations, we further performed cell cycle analyses. In Fig. 3a and b, the ratios of multinucleated cells (DNA content >4N) were increased by transfection of Aurora-B-siRNA in U251MG (22.7%), T98G (17.1%), and Saos-2 (8.9%) cells, compared with their controls (8.7%, 6.0%, and 2.1%), respectively. The ratios of G2/M phase were also increased by transfection of Aurora-B-siRNA in U251MG, T98G, and Saos-2 cells. However, we observed no significant differences in the ratios of multinucleated cells and G2/M phase in U87MG cells (wild-type p53) between transfections of Aurora-B- and control-siRNA. Moreover, transfection of Aurora-B-siRNA in *p53* gene-transduced Saos-2 cells did not increase the ratios of multinucleated cells significantly as well as in U87MG cells (Fig. 3b).

Reinforcement of anti-tumor effect of TMZ by inhibiting Aurora-B function

We investigated the reinforcement of the anti-tumor effect of TMZ by inhibiting Aurora-B function. The results are shown in Fig. 4. In U251MG cells, an approximately 50% inhibition in cell viability was

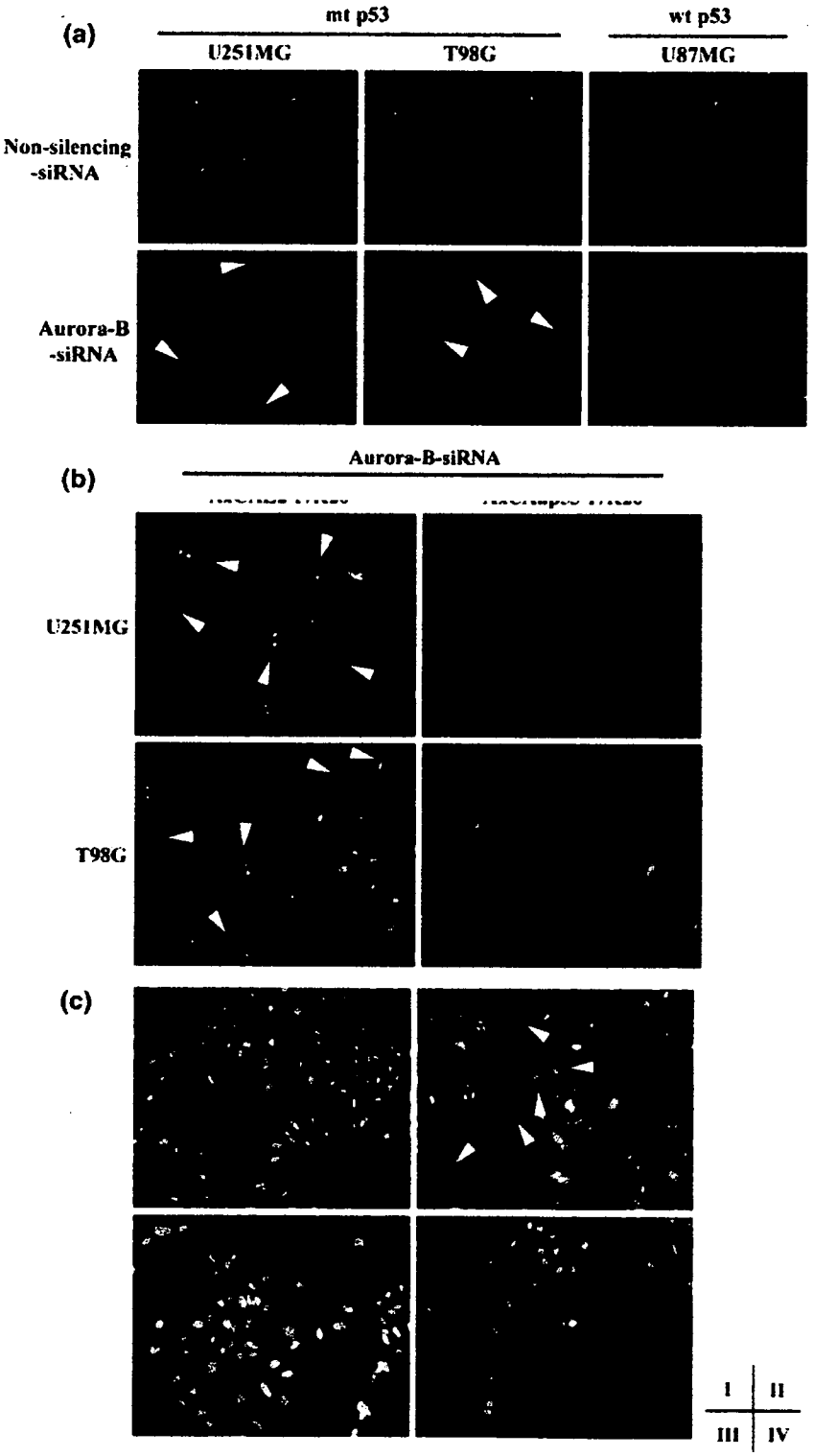

demonstrated by adding TMZ alone. However, significant inhibition was detected with combined treatment of Aurora-B-siRNA and TMZ, compared with each material alone ($^*P < 0.05$). T98G cells also showed a dramatic inhibition with the combined treatment compared with each material alone ($^*P < 0.05$). Of the three glioma cell lines, U87MG cells were most sensitive to TMZ (approximately 55% inhibition by TMZ alone), and the combined treatment also demonstrated sensitive response (approximately 60% inhibition). No significant differences were detected among the treatments tested in U87MG cells.

◀ **Fig. 2** Morphological changes of the nuclei after inhibition of Aurora-B function. (**a**) Human glioma cells. An increased number of multinucleated cells (white arrowhead) was obtained 48 h after transfection of Aurora-B-siRNA in U251MG and T98G cells, however there was no increase in the number of them in Aurora-B inhibited U87MG cells. (Magnifications: ×200; wt: wild type; mt: mutant type) (**b**) Morphological changes of the nuclei in human glioma cells with mutant type p53. We transduced AxCAZ2-F/K20 or AxCAhp53-F/K20 for 24 h, followed by transfection of Aurora-B-siRNA for 48 h into U251MG and T98G cells with mutant type p53. An increase in the number of multinucleated cells (white arrowhead) was observed in the *LacZ* transduced cells. On the other hand, we detected a remarkable reduction in the number of them in the *p53* gene-transduced cells. (Magnifications: ×200) (**c**) Morphological changes of the nuclei in human osteosarcoma cells with p53-null. To investigate the multinucleated cells associated with Aurora-B and p53 dysfunction, we also transduced AxCAhp53-F/K20 for 24 h, followed by transfection of Aurora-B-siRNA for 48 h into Saos-2 cells with p53-null. An increase in the number of multinucleated cells (white arrowhead) was shown in Aurora-B inhibited Saos-2 cells, and the failure of chromosome arrangement was also demonstrated (white circle). However, we observed no increase in the number of multinucleated cells not only in the *p53* gene-transduced Saos-2 cells, but also in the *p53* gene-transduced/Aurora-B inhibited Saos-2 cells. (Magnifications: ×200, I: untreated, II: Aurora-B-siRNA, III: AxCAhp53-F/K20, IV: AxCAhp53-F/K20 and Aurora-B-siRNA)

Discussion

We investigated the relationships among multinucleated cells, p53, Aurora-B and anti-tumor effect of TMZ in the present study. The principal findings are that the inhibition of Aurora-B function led to increase in the number of multinucleated cells and the ratios of G2/M phase in p53-mutant and p53–null cells, but not in p53-wild cells or the cells transduced adenovirally with wild-p53, and that the combination of TMZ and inhibition of Aurora-B function remarkably induced the cell death in human glioma cells, even in *p53* gene deficient and TMZ-resistant glioma cells.

Multinucleated cells

Since both U251MG and T98G cells have mutant type p53 and U87MG cells have wild type p53, we first investigated the role of p53 in association with Aurora-B function in these glioma cells. Our results demonstrated increases in the number of multinucleated cells and the ratios of G2/M phase 48 h after transfection of Aurora-B-siRNA in U251MG and T98G cells, but no significant differences in U87MG cells. In addition, *p53* gene-transduced U251MG and T98G cells showed no increase in the number of multinucleated cells after Aurora-B inhibition. To further investigate these relationships, we used Saos-2 cells with p53-null. After Aurora-B inhibition, Saos-2 cells showed an increase in the number of multinucleated cells, while *p53* gene-transduced Saos-2 cells did not. Aurora-B protein is induced during G2/M phase and its inhibition leads to a failure of cytokinesis and subsequently no entry beyond G2/M phase, eventually to the formation of multinucleated cells [35]. Our results of the cells with mutant type p53 and p53-null are consistent with these results, however those with p53 wild type are not. Additionally, in our clinical samples of giant cell glioblastoma, molecular genetic analysis revealed that multinucleated giant cells showed the dysfunction of Aurora-B and p53 mutation. Here we focused on p53 that plays an important role in cell cycle. p53 is critical for G1 arrest in response to DNA damage [36, 37], and is required to prevent polyploidization following mitotic spindle damage [38, 39], and results in participation in the maintenance of euploidy [40]. On the other hand, p53 is also associated with G2 arrest mediated by 14-3-3σ. After DNA damage, 14-3-3σ is activated by p53 and maintains G2 checkpoint [41]. It has been also reported that polypoidization and subsequent aneuploidization are prevented by the function of the mitotic spindle checkpoint, a p53-dependent G1 checkpoint and an additional G2 checkpoint [42]. Thus, p53 may be a key molecule to maintain euploidy and to prevent the formation of multinucleated cells. Consequently, we suggest that the formation of multinucleated cells requires not only dysfunction of Aurora-B but also that of p53.

Cell death

TMZ is an alkylating agent that has been commonly used in treatment of malignant gliomas. Recently, we have reported that interferon (IFN)-β down-regulates MGMT mediated by p53 protein, and sensitizes resistant glioma cells to TMZ and down-regulates MGMT expression. Methylation of the MGMT promotor is a useful predictor of the sensitivity to alkylating agents [34]. In the present study, we examined further whether the anti-tumor effect of TMZ is able to be enhanced against TMZ-resistant glioma cells using Aurora-B-siRNA resulting in the formation of multinucleated cells. U251MG and T98G cells, the human glioma cells with mutant type p53, demonstrated moderate resistance and severe resistance, respectively. In our previous study, U251MG cells showed methylated MGMT, whereas T98G cells had unmethylated MGMT. These findings may explain the difference in the sensitivity to TMZ between these two glioma cell lines [34]. However, we detected significant inhibitions in cell viability in both the human glioma cells with mutant type p53 by

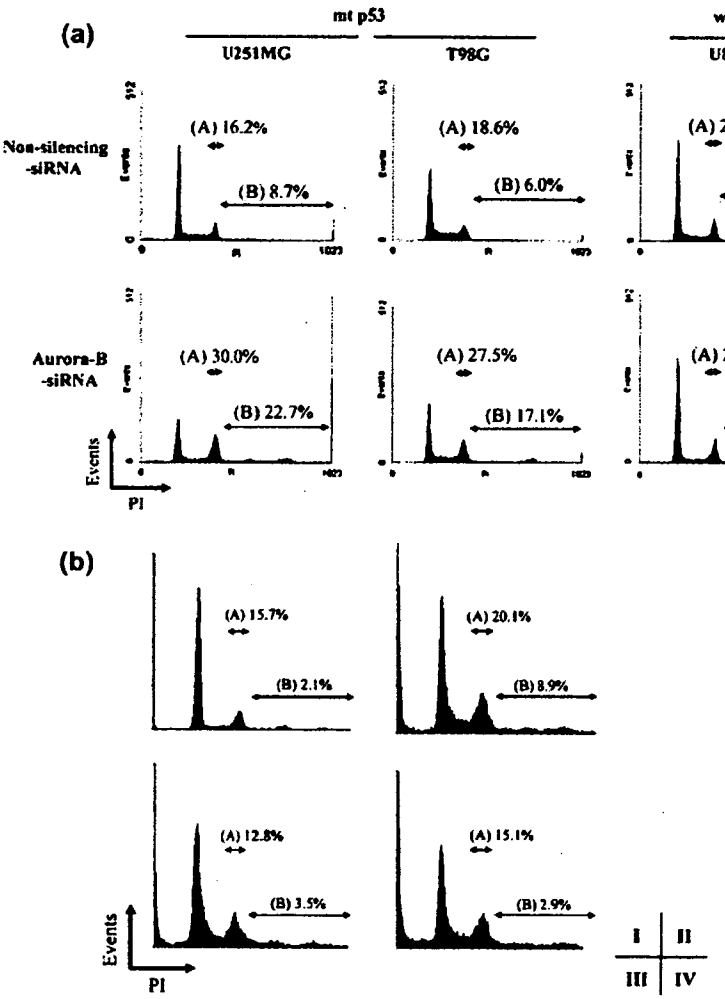

Fig. 3 Cell cycle analysis. (**a**) Human glioma cells. Increase in the number of multinucleated cells and the ratios of G2/M phase by inhibiting Aurora-B function. These results showed remarkable increases in both ratios of G2/M phase (A) and multinucleated cells (B) in U251MG and T98G cells (mutant type p53) 48 h after transfection of Aurora-B-siRNA. However, no significant differences between transfections of Aurora-B- and non-silencing-siRNA were observed in U87MG cells (wild type p53). (wt: wild type; mt: mutant type) (**b**) Multinucleated cells and G2/M phase in human osteosarcoma cells. In Saos-2 cells with p53-null, 48 h after transfection of Aurora-B-siRNA, the number of multinucleated cells and the ratio of G2/M phase increased. However, we observed no increase in the number of multinucleated cells not only in the *p53* gene-transduced Saos-2 cells, but also in the *p53* gene-transduced/Aurora-B inhibited Saos-2 cells. (I: untreated, II: Aurora-B-siRNA, III: AxCAhp53-F/K20, IV: AxCAhp53-F/K20 and Aurora-B-siRNA)

the combined treatment of TMZ and inhibition of Aurora-B function. In particular, the combined treatment demonstrated an approximately 60% inhibition in cell viability even in T98G cells that showed the highest resistance to TMZ alone (approximately 20% inhibition). On the other hand, we observed no significant difference between TMZ alone and the combined treatment in U87MG cells, the glioma cells with wild type p53. These results suggest that the inhibition of Aurora-B function sensitizes resistant glioma cells with mutant type p53 to TMZ regardless of MGMT methylation or unmethylation. In the present study, inhibition of Aurora-B function led to the formation of the multinucleated cells in mutant type p53 and p53-null cells, but not in wild type p53 cells. Furthermore, in our clinical samples of giant cell glioblastomas, all of them showed p53 mutation and better overall survivals than typical glioblastomas in spite of MGMT unmethylated status. Here we considered the relationship between p53 and cell death; it has been reported that 14-3-3σ, activated by p53, prevents mitotic death ('mitotic catastrophe') [41]. Moreover, according to the relationship between multinucleated cells and cell death, the multinucleated cells are unable to divide further, followed by cell death in Aurora-B inactivated cells [35]. In addition, the proliferation studies of glioblastomas have demonstrated that large, multinucleated cells are generally non-proliferating [18, 22]. In other

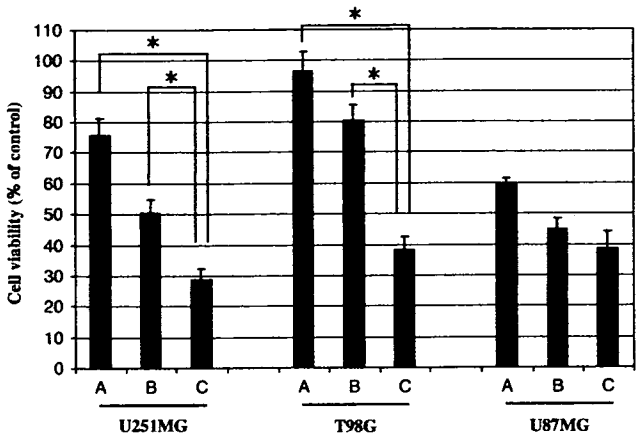

Fig. 4 The reinforcement of anti-tumor effect of TMZ combined with Aurora-B-siRNA. U251MG (mutant p53): Administration of TMZ alone resulted in an approximately 50% inhibition in cell viability. In addition, the combined treatment of Aurora-B-siRNA and TMZ showed a significant inhibition in cell viability compared with each material alone (* $P < 0.05$). T98G (mutant p53): The strong resistance against TMZ alone was observed, however the combined treatment demonstrated a significant inhibition in cell viability, approximately 60% inhibition, compared with each material alone (*$P < 0.05$). U87MG (wild type p53): U87MG cells showed more sensitivity to TMZ alone than the other two glioma cells, and the combined treatment demonstrated sensitivity as well. Aurora-B-siRNA alone also demonstrated the highest inhibition in cell viability of these glioma cells. These numbers were expressed as ratios compared with non-silencing-siRNA control. (A: Aurora-B-siRNA, B: TMZ (100 μM), C: combined treatment)

clinical cases, the degree of malignancy in giant cell glioblastoma was determined by the biological behavior of the mononucleated giant cells and small cells, not by that of the multinucleated giant cells [43]. In the present study, TMZ was administered at the time of the increase in the number of multinucleated cells in U251MG and T98G cells with mutant type of p53, therefore TMZ may show higher sensitivity to the multinucleated cells rather than to the mononucleated cells, under p53 deficient status. In contrast, U87MG cells with wild type p53 showed the highest sensitivity to TMZ alone of these glioma cells tested and no increase in the formation of multinucleated cells by inhibiting Aurora-B function, therefore it is possible that there was no enhancement of the anti-tumor effect of TMZ in U87MG cells even with the combined treatment. On the other hand, Aurora-B-siRNA alone inhibited cell viabilities in U251MG and U87MG cells, particularly in the latter. Aurora-B is essential for cell viability and required for proper progression of cytokinesis in mammalian cells [35], however its overexpression has been observed in many human cancer cells [6, 44]. These findings suggest that proper expression of Aurora-B may be indispensable to the life of cells. In the present study, U87MG cells showed a proper progression of cytokinesis without an increase in the formation of multinucleated cells. Therefore, U87MG cells may properly express Aurora-B to maintain their own cell viabilities, and may have demonstrated the highest inhibition in cell viability by Aurora-B inhibition alone.

Conclusions

We suggest that the formation of multinucleated cells requires not only dysfunction of Aurora-B but also that of p53, and that multinucleation can lead to cell death. The combined treatment of TMZ and inhibition of Aurora-B function indicated a remarkable inhibition in cell viability even against TMZ resistant glioma cells without p53 function. Consequently, this treatment may be developed into a crucial therapy for malignant gliomas.

Acknowledgements We thank Professor Hirofumi Hamada, Department of Molecular Medicine, Sapporo Medical University, for providing adenoviral vectors. This manuscript was supported in part by Grants-in-Aid for Scientific Research 16209044 and 16390408 from the Japan Society for the Promotion of Science.

References

1. Albertson DG, Collins C, McCormick F, Gray JW (2003) Chromosome aberrations in solid tumors. Nat Genet 34:369–376
2. Jallepalli PV, Lengauer C (2001) Chromosome segregation and cancer: cutting through the mystery. Nat Rev Cancer 1:109–117
3. Doxsey S (1998) The centrosome—a tiny organelle with big potential. Nat Genet 20:104–106
4. Bischoff JR, Plowman GD (1999) The Aurora/Ipl1p kinase family: regulators of chromosome segregation and cytokinesis. Trends Cell Biol 9:454–459
5. Giet R, Prigent C (1999) Aurora/Ipl 1p-related kinases, a new oncogenic family of mitotic serine-threonine kinases. Cell Sci 112:3591–3601
6. Nigg EA (2001) Cell division mitotic kinases as regulators of cell division and its checkpoints. Nature Rev Mol Cell Biol 2:21–32
7. Sugimoto K, Urano T, Zushi H, Inoue K, Tasaka H, Tachibana M, Dotsu M (2002) Molecular dynamics of Aurora-A kinase in living mitotic cells simultaneously visualized with histone H3 and nuclear membrane protein importinα. Cell Struct Funct 27:457–467
8. Berdnik D, Knoblich JA (2002) Drosophila Aurora-A is required for centrosome maturation and actin-dependent asymmetric protein localization during mitosis. Curr Biol 12:640–647
9. Kufer TA, Nigg EA, Silljé HH (2003) Regulation of Aurora-A kinase on the mitotic spindle. Chromosoma 112:159–163
10. Bischoff JR, Anderson L, Zhu Y, Mossie K, Ng L, Souza B, Schryver B, Flanagan P, Clairvoyant F, Ginther C, Chan CS, Novotny M, Slamon DJ, Plowman GD (1998) A homologue of Drosophila aurora kinase is oncogenic and amplified in human colorectal cancers. EMBO J 17:3052–3065

11. Murata-Hori M, Wang Y-L (2002) Both midzone and astral microtubules are involved in the delivery of cytokinesis signals: insights from the mobility of aurora B. J Cell Biol 159:45–53
12. Adams RR, Carmena M, Earnshaw WC (2001) Chromosomal passengers and the (aurora) ABCs of mitosis. Trends Cell Biol 11:49–54
13. Kimura M, Matsuda Y, Yoshioka T, Sumi N, Okano Y (1998) Identification of STK12/Aik2: a human gene related to aurora of Drosophila and yeast IPL1. Cytogenet Cell Genet 82:147–152
14. Zhao X, He M, Wan D, Ye Y, He Y, Han L, Guo M, Huang Y, Qin W, Wang MW, Chong W, Chen J, Zhang L, Yang N, Xu B, Wu M, Zuo L, Gu J (2003) The minimum LOH region defined on chromosome 17p13.3 in human hepatocellular carcinoma with gene content analysis. Cancer Lett 190:221–232
15. Tatsuka M, Katayama H, Ota T, Tanaka T, Odashima S, Suzuki F, Terada Y (1998) Multinuclearity and increased ploidy caused by overexpression of the aurora- and Ipl1-like midbody-associated protein mitotic kinase in human cancer cells. Cancer Res 58:4811–4816
16. Kimura M, Matsuda Y, Yoshioka T, Okano Y (1999) Cell Cycle-dependent expression and centrosome localization of a third human Aurora/Ipl1-related protein kinase, AIK3. J Biol Chem 274: 7368–7378
17. Homma T, Fukushima T, Vaccarella S, Yonekawa Y, Di Patre PL, Franceschi S, Ohgaki H (2006) Correlation among pathology, genotype, and patient outcomes in glioblastoma. J Neuropathol Exp Neurol 65: 846–854
18. Meyer-Puttlitz B, Hayashi Y, Waha A (1997) Molecular genetic analysis of giant cell glioblastomas. Am J Pathol 151:853–857
19. Muller W, Slowik F, Firsching R (1987) Contribution to the problem of giant cell astrocytomas. Neurosurg Rev 10:213–219
20. Palma L, Celli P, Maleci A (1989) Malignant monstrocellular brain tumours. A study of 42 surgically treated cases. Acta Neurochir 97:17–25
21. Peraud A, Watanabe K, Plate KH, Yoneyama Y, Kleihues P, Ohgaki H (1997) p53 mutations versus EGF receptor expression in giant cell glioblastomas. J Neuropathol Exp Neurol 56(11):1236–1241
22. Giangaspero F, Doglioni C, Rivano MT (1987) Growth fraction in human brain tumors defined by the monoclonal antibody Ki-67. Acta Neuropathol 74:179–182
23. Fujita M, Mizuno M, Nagasaka T, Wakabayashi T, Maeda K, Ishii D, Arima T, Kawajiri A, Inagaki M, Yoshida J (2004) Aurora-B dysfunction of multinucleated giant cells in glioma detected by site-specific phosphorylated antibodies. J Neurosurg 101:1012–1017
24. Maeda K, Mizuno M, Wakabayashi T, Takasu S, Nagasaka T, Inagaki M, Yoshida J (2003) Morphological assessment of the development of multinucleated giant cells by using mitosis-specific phosphorylated antibodies. J Neurosurg 98:854–859
25. Tada M, Iggo RD, Waridel F, Nozaki M, Matsumoto R, Sawamura Y, Shinohe Y, Ikeda J, Abe H (1997) Reappraisal of p53 mutations in human malignant astrocytic neoplasms by p53 functional assay: comparison with conventional structural analyses. Mol Carcinog 18:171–176
26. Levine AJ (1997) p53, the cellar gatekeeper for growth and division. Cell 88:323–331
27. Helton ES, Chen X (2006) p53 modulation of the DNA damage response. J Cell Biochem 1 Oct 9 (in press)
28. Asaoka K, Tada M, Sawamura Y, Ikeda J, Abe H (2000) Dependence of efficient adenoviral gene delivery in malignant glioma cells on the expression levels of the Coxsackievirus and adenovirus receptor. J Neurosurg 92:1002–1008
29. Mondal AM, Chinnadurai S, Datta K, Chauhan SS, Sinha S, Chattopadhyay P (2006) Identification and functional characterization of a novel unspliced transcript variant of HIC-1 in human cancer cells exposed to adverse growth conditions. Cancer Res 66: 10466–10477
30. Okamura H, Yoshida K, Morimoto H, Hanaji T (2005) PTEN expression elicited by EGR-1 transcription factor in calyculin A-induced apoptotic cells. J Cell Biochem 94(1):117–125
31. Hauf S, Cole RW, LaTerra S, Zimmer C, Schnapp G, Walter R, Heckel A, van Meel J, Rieder CL, Peters JM (2003) The small molecule Hesperadin reveals a role for Aurora B in correcting kinetochore-microtubule attachment and in maintaining the spindle assembly checkpoint. J Cell Biol 161:281–294
32. Yamamoto S, Yoshida Y, Aoyagi M, Ohno K, Hirakawa K, Hamada H (2002) Reduced transduction efficiency of adenoviral vectors expressing human *p53* gene by repeated transduction into glioma cells in *vitro*. Clin Cancer Res 8:913–921
33. Fults D, Brockmeyer D, Tullous MW, Pedone CA, Cawthon RM (1992) p53 mutation and loss of heterozygosity on chromosomes 17 and 10 during human astrocytoma progression. Cancer Res 52:674–679
34. Natsume A, Ishii D, Wakabayashi T, Tsuno T, Hatano H, Mizuno M, Yoshida J (2005) IFN-β down-regulates the expression of DNA repair gene MGMT and sensitizes resistant glioma cells to temozolomide. Cancer Res 65:7573–7579
35. Terada Y, Tatsuka M, Suzuki F, Yasuda Y, Fujita S, Otsu M (1998) AIM-1: a mammalian midbody-associated protein required for cytokinesis. EMBO J 17:667–676
36. Cox LS, Lane DP (1995) Tumor suppressors, kinases, clamps how p53 regulates the cell cycle in response to DNA damage. BioEssays 17:501–508
37. Kastan MB, Zhan Q, el-Deiry WS, Carrier F, Jacks T, Walsh WV, Plunkett BS, Vogelstein B, Fornace AJ Jr (1992) A mammalian cell cycle checkpoint pathway utilizing p53 and CADD45 is detective in ataxia-telangiectasia. Cell 71:587–597
38. Lanni JS, Jacks T (1998) Characterization of the p53-dependent postmitotic checkpoint following spindle disruption. Mol Cell Biol 18:1055–1064
39. Minn AJ, Boise LH, Thompson CB (1996) Expression Bcl-x and loss of p53 can cooperate to overcome a cell cycle checkpoint induced by mitotic spindle damage. Genes Dev 10:2621–2631
40. Harvey M, Sands AT, Weiss RS, Hegi ME, Wiseman RW, Pantazis P, Giovanella BC, Tainsky MA, Bradley A, Donehower LA (1993) In vitro growth characteristics of embryo fibroblasts isolated from p53-deficient mice. Oncogene 8:2457–2467
41. Chan TA, Hermeking H, Lengauer C, Kinzler KW, Vogelstein B (1999) 14-3-3σ is required to prevent mitotic catastrophe after DNA damage. Nature (London) 401:616–620
42. Vogel C, Kienitz A, Hofmann I, Müller R, Bastians H (2004) Crosstalk of the mitotic spindle assembly checkpoint with p53 to prevent polyploidy. Oncogene 23:6845–6853
43. Huang MC, Kubo O, Tajika Y (1996) A clinico-immunohistochemical study of giant cell glioblastoma. Noshuyo Byori 13:11–16
44. Katayama H, Brinkley WR, Sen S (2003) The Aurora kinases: role in cell transformation and tumorigenesis. Cancer Metastasis Rev 22(4):451–464

脳神経外科速報 vol.17 no.8 936～944, 2007

肺癌脳転移に対するゲフィチニブの効果

島戸真司[1] 若林俊彦[2] 光冨徹哉[3] 吉田 純[4]

Shinji SHIMATO, Toshihiko WAKABAYASHI, Tetsuya MITSUDOMI, Jun YOSHIDA

1) 岐阜県立多治見病院脳神経外科 〒507-8522 岐阜県多治見市前畑町5-161
2) 名古屋大学附属病院遺伝子再生医療センター
3) 愛知県がんセンター中央病院胸部外科
4) 名古屋大学医学部脳神経外科

Ⅰ．はじめに

ゲフィチニブ（イレッサ®）は，上皮成長因子受容体（EGFR）のチロシンキナーゼ（TK）を標的とする分子標的治療薬である．ゲフィチニブは，日本も参加したプラチナ製剤を含む前化学療法無効ないし再発進行非小細胞肺癌に対する第2相の国際共同試験（IDEAL1，2）で9～18％ほどの奏効率が報告され，特に日本人では27.5％の奏効率が認められたことを受け[9, 18]，2002年7月に厚生労働省より手術不能または再発非小細胞肺癌に対してわが国において世界で初めて承認された．使用開始後，当初予想していなかった有害事象として致死的な急性肺傷害を起こす症例があり，薬害の話題として社会的問題となったが，他の抗癌剤で無効でも劇的な効果を示しその恩恵を受ける患者も多く，現在も肺癌治療において重要な薬物の一つとして使用されている．

転移性脳腫瘍は脳神経外科医が最も多く遭遇する脳腫瘍であり，原発巣としては肺癌が約半数を占める．現在の転移性脳腫瘍に対する治療としては，手術摘出あるいは放射線による治療の効果が広く認められ標準となっている．他方，抗癌剤治療についてはblood-brain-barrier（BBB）によって薬剤が浸透しにくいこともあり，効果は限られているのが現状である[32]．その中で，ゲフィチニブの登場以後，脳転移に対しての著効例が報告されるようになった．今回は，ゲフィチニブの特徴と現在までに得られている知見について触れた後，脳転移例に対する有効性について文献レビューを中心にまとめ，また脳神経外科領域に関連する話題としてグリオーマに対する治療の可能性についても，EGFRとの関係を中心に分子生物学的視点を含め概説する．

Ⅱ．EGFRおよびゲフィチニブの作用機序

EGFRは体内のさまざまな細胞で分化，増殖等において重要な働きをしているが，種々の悪性腫瘍細胞でも発現がみられ，腫瘍細胞における悪性化へ強く関与し，その過剰発現は予後不良因子である[33]．EGFRの構造は，細胞外領域，細胞膜貫

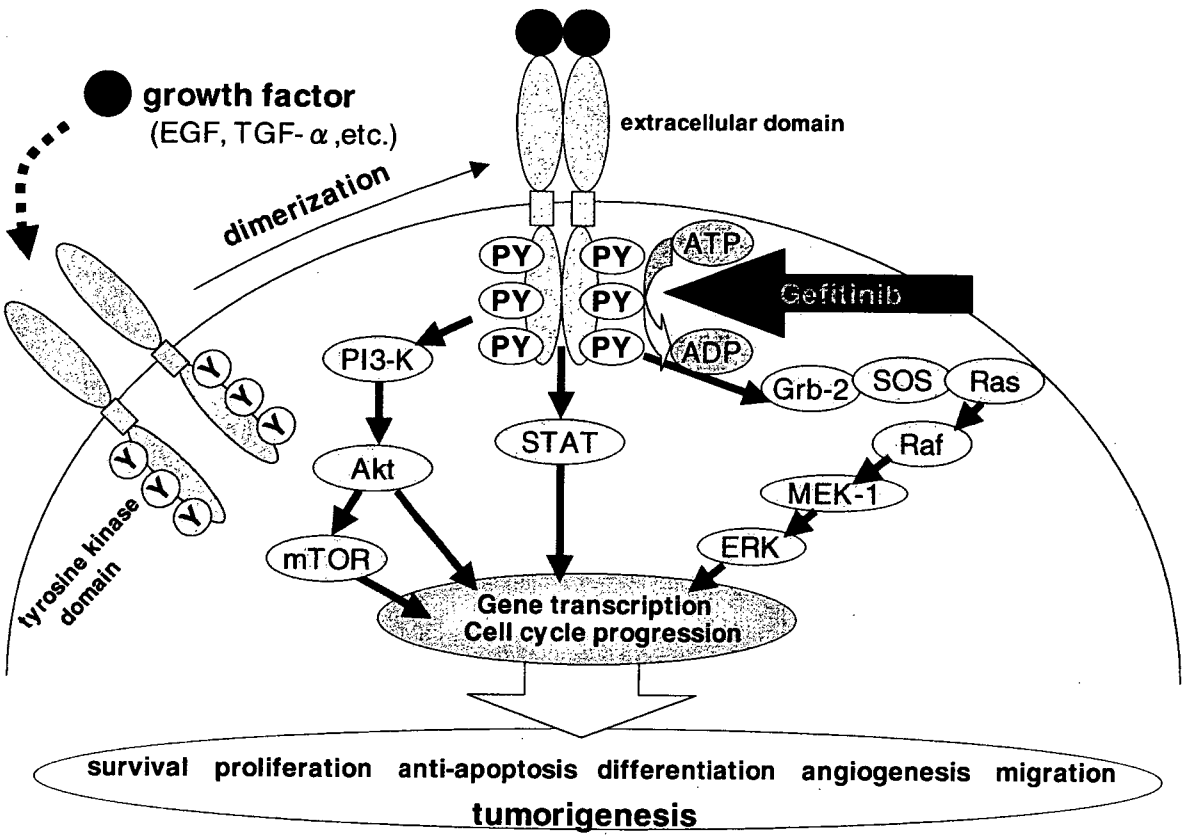

図1　EGFR活性化によるシグナル伝達とゲフィチニブ作用部位
リガンドであるEGF，TGFα等がEGFR細胞外領域に結合すると，EGFRや同じファミリーに属するerbB2/HER2，erbB3/HER3，erbB4/HER4とホモあるいはヘテロダイマーを形成し，細胞内領域のTKはお互いのチロシン残基をリン酸化して活性化される．腫瘍細胞では，EGFRがリガンド非依存性に恒常的に活性化され，RAS-MAPK経路，PI3K-Akt経路，STAT経路などに伝えられ，腫瘍細胞の増殖，アポトーシスの回避，血管新生，転移などに寄与し，悪性化に関与する．ゲフィチニブはEGFRの細胞内領域のTKにおけるATP結合を競合的に阻害することで抗腫瘍効果を発揮する．

通領域，およびTK部位を有する細胞内領域からなる．細胞外領域のリドカイン結合部位にEGFやTGFαなどのリガンドが結合すると，EGFR細胞内領域のTK部位にATPが結合し自己リン酸化して活性化され，RAS-MAPK経路，PI3K-AKT経路，STAT経路などにシグナルが伝わり，腫瘍細胞における増殖，浸潤・転移形成への関与，血管新生にかかわる分子発現やアポトーシス抑制に密接に働くと考えられている[1]．

ゲフィチニブはEGFR-TKの自己リン酸化部位へのATP結合を競合的に阻害し，以下へのシグナル伝達を阻害することで抗腫瘍効果を発揮する（図1）．EGFRのTK阻害薬という薬効のみで，非小細胞肺癌に対して大きな臨床効果が得られる可能性が示され，当初世界中で注目され大きな期待が寄せられた薬剤である．